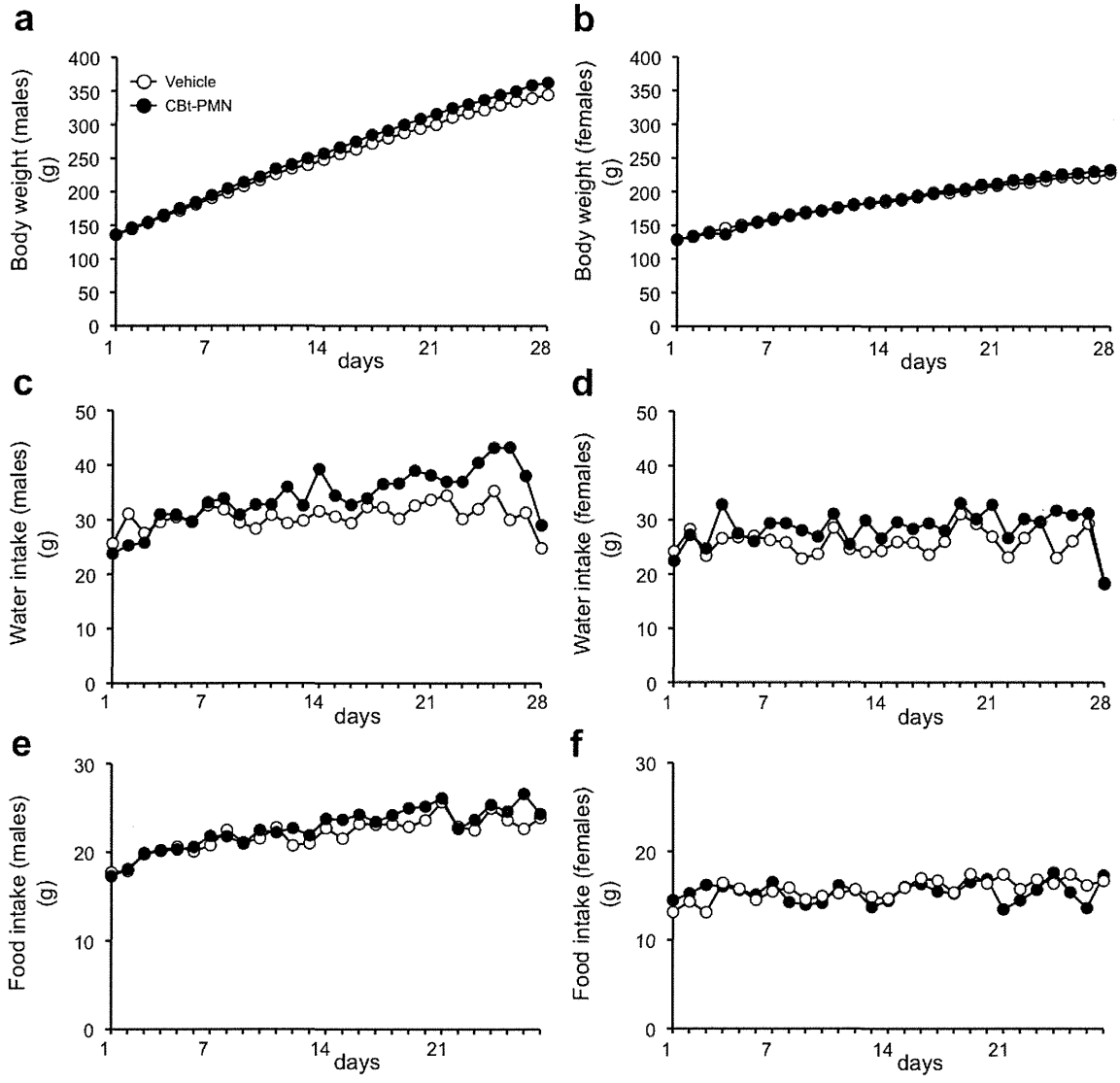

Figure S5. Body weight gain, water intake change, and food intake change of male or female SD rats treated with oral administration of vehicle or CBt-PMN (**11b**) at 30 mg/kg/day for 28 consecutive days (n = 6). **a**–**b**) Body weight gain. **c**–**d**) Water intake change. **e**–**f**) Food intake change. Males: **a**, **c**, and **e**. Females: **b**, **d**, and **f**. Open and closed circles indicate vehicle and CBt-PMN (**11b**) treatment, respectively.

Table S3. Plasma parameters of male ICR mice after oral administration of vehicle or CBt-PMN (**11b**) at 30 mg/kg/day for 7 consecutive days (n = 7–8)

	Vehicle	NEt-TMN (**5**)	CBiM-PMN (**11a**)	CBt-PMN (**11b**)
AST (U/l)	50.5 ± 5.6	87.9 ± 18.9 *	51.3 ± 3.9	48.9 ± 3.0
ALT (U/l)	21.4 ± 1.5	43.5 ± 6.0 **	32.7 ± 6.4	21.9 ± 0.7
γ-GTP (U/l)	7.9 ± 0.8	7.1 ± 0.3	6.4 ± 0.3	6.5 ± 0.2
ALP (U/l)	305.1 ± 27.1	968.9 ± 115.0 **	456.0 ± 51.5	391.9 ± 37.5
CRE (mg/dL)	0.1 ± 0.0	0.1 ± 0.0	0.1 ± 0.0	0.1 ± 0.0
BUN (mg/dL)	25.1 ± 1.4	26.0 ± 1.8	24.1 ± 2.1	25.1 ± 1.9
GLU (mg/dL)	107.5 ± 9.8	177.8 ± 8.8 **	125.7 ± 7.2	95.6 ± 4.2

AST : Alanine aminotransferase, ALT : aspartate aminotransferase, γ-GTP : γ-glutamyl transpeptidase, ALP : alkaline phosphatase, CRE : creatinine, BUN : blood urea nitrogen, GLU : glucose.

Data are mean ± s.e.m.; Statistical analysis was performed by analysis of variance (ANOVA). Significant differences: * $p < 0.05$ vs. vehicle. ** $p < 0.01$ vs. vehicle.

Table S4. Organ weights of male or female SD rats after oral administration of vehicle or CBt-PMN (**11b**) at 30 mg/kg/day for 28 consecutive days (n = 6)

	Males		Females	
	Vehicle	CBt-PMN (**11b**)	Vehicle	CBt-PMN (**11b**)
Weight (g)	324.3 ± 8.7	337.8 ± 4.6	213.4 ± 2.1	216.1 ± 10.7
Brain (g)	2.0 ± 0.1	2.0 ± 0.1	1.8 ± 0.0	1.7 ± 0.0
Liver (g)	9.7 ± 0.6	9.7 ± 0.4	5.9 ± 0.2	6.2 ± 0.4
Kidney (g)	2.5 ± 0.1	2.6 ± 0.1	1.6 ± 0.0	1.5 ± 0.1
Spleen (g)	0.6 ± 0.0	0.7 ± 0.1	0.4 ± 0.0	0.5 ± 0.0
Testis (g)	3.9 ± 0.2	4.5 ± 0.1 *		

Data are mean ± s.e.m.; Statistical analysis was performed by analysis of variance (ANOVA). Significant differences: * $p < 0.05$ vs. vehicle.

Table S5. Hematological and plasma parameters of male and female SD rats after oral administration of vehicle or CBt-PMN (**11b**) at 30 mg/kg/day for 28 consecutive days (n = 6)

	Males			Females		
	vehicle	CBt-PMN	Reference[c]	vehicle	CBt-PMN	Reference[c]
WBC ($\times 10^2$/mL)[a]	71.7 ± 4.2	92.5 ± 18.6	–	76.5 ± 9.3	72.5 ± 7.5	–
RBC ($\times 10^4$/mL)[a]	741.8 ± 17.4	746.2 ± 11.7	–	778.3 ± 18.1	767.3 ± 12.0	–
PLT ($\times 10^4$/mL)[a]	123.3 ± 5.7	139.9 ± 13.1	–	129.3 ± 4.9	140.3 ± 7.1	–
HGB (g/dL)[a]	14.8 ± 0.2	14.4 ± 0.2	14.4 – 16.0	14.7 ± 0.2	14.5 ± 0.2	13.7 – 15.7
HCT (%)[a]	45.5 ± 0.6	45.0 ± 0.7	41.2 – 47.3	45.7 ± 0.8	44.8 ± 0.6	9.6 – 46.0
MCV (fL)[a]	61.4 ± 0.8	60.4 ± 0.4	53.0 – 59.5	58.7 ± 0.6	58.4 ± 0.6	53.6 – 58.1
MCH (pg)[a]	20.0 ± 0.2	19.3 ± 0.2 *	18.3 – 20.0	18.9 ± 0.3	18.9 ± 0.2	18.6 – 20.0
MCHC (g/dL)[a]	32.5 ± 0.1	31.9 ± 0.2 *	32.7 – 35.7	32.2 ± 0.3	32.2 ± 0.1	32.8 – 36.2
AST (U/l)[b]	65.7 ± 3.5	75.2 ± 2.8 *	87.0 – 114.0	60.2 ± 1.6	64.8 ± 2.0 *	85.0 – 123.0
ALT (U/l)[b]	27.8 ± 1.4	37.7 ± 2.0 **	28.0 – 40.0	21.5 ± 2.1	29.3 ± 1.9 **	25.0 – 36.0
γ-GTP (U/l)[b]	8.2 ± 0.4	8.3 ± 0.2	0.0 – 1.0	8.3 ± 0.2	8.7 ± 0.3	0.0 – 0.4
ALP (U/l)[b]	585.7 ± 34.3	607.5 ± 39.7	136.0 – 188.0	434.3 ± 50.7	476.5 ± 75.2	90.0 – 147.0
CRE (mg/dL)[b]	0.2 ± 0.0	0.2 ± 0.0	0.5 – 0.6	0.3 ± 0.0	0.3 ± 0.0	0.5 – 0.6
BUN (mg/dL)[b]	16.4 ± 0.7	11.8 ± 0.4 **	13.0 – 16.0	13.8 ± 0.7	14.5 ± 0.9	11.0 – 16.0
TG (mg/dL)[b]	44.8 ± 2.8	50.8 ± 2.9	61.0 – 99.0	55.0 ± 4.9	77.5 ± 5.5 **	42.0 – 74.0
TCHO (mg/dL)[b]	56.2 ± 7.5	34.0 ± 4.5 *	54.0 – 74.0	25.7 ± 3.7	44.8 ± 10.6	67.0 – 87.0
GLU (mg/dL)[b]	181.2 ± 16.1	149.8 ± 17.7	112.0 – 176.0	118.3 ± 5.7	145.5 ± 10.6 *	113.0 – 185.0

a. Measured with a pocH-100i (Sysmex).

b. Measured with a Fuji Dry Chem 4000V (Fuji Medical Co., Tokyo, Japan).

c. These data were cited from the Clinical Laboratory Parameters for Crl:CD(SD) Rats (CRL_Mar,2006) by Charles River®.

Data are mean ± s.e.m.; Statistical analysis was performed by analysis of variance (ANOVA). Significant differences: * $p < 0.05$ vs. vehicle. ** $p < 0.01$ vs. vehicle.

Table S6. Primer list

Primer		Sequence
Irs1	Forward	5'-CAAGACGCTCCAGTGAGGATTTAAG-3'
	Reverse	5'-AGACGTGAGGTCCTGGTTGTGA-3'
Irs2	Forward	5'-TGGTTCTCACAAGAGTTCCAGCA-3'
	Reverse	5'- AGCTATTGGGACCACCACTCCTAA-3'
Slc2a1	Forward	5'-TGTGGGCATGTGCTTCCAGTA-3'
	Reverse	5'-GCCTTTGGTCTCAGGGACTTTG-3'
Slc2a2	Forward	5'-GGCATCAGCCAGCCTGTGTA-3'
	Reverse	5'-CATGCCAATCATCCCGGTTAG-3'
G6Pc	Forward	5'-CAGCAACAGCTCCGTGCCTA-3'
	Reverse	5'-TCCCAACCACAAGATGACGTTC-3'
Pck	Forward	5'-TCTTTGGTGGCCGTAGACCTG-3'
	Reverse	5'-GCCAGGTATTTGCCGAAGTTGTAG-3'
Gck	Forward	5'-CGGTGAGCTGGACGAGTTC-3'
	Reverse	5'-ACCAGCTCGCCCATGTACTT-3'
Scd1	Forward	5'-TCCGGAACCGAAGTCCAC-3'
	Reverse	5'-GTGGTCGTGTAAGAACTGGAGATCT-3'
Fasn	Forward	5'-ATTGGCTCCACCAAATCCAAC-3'
	Reverse	5'-CCCATGCTCCAGGGATAACAG-3'
Srebp1c	Forward	5'-GGTTTTGAACGACATCGAAGA-3'
	Reverse	5'-CGGGAAGTCACTGTCTTGGT-3'

5. REFERENCES

S1. M.F. Boehm, *et al. J. Med. Chem.*, **1994**, *37*, 2930–2941.
S2. S. Fujii, *et al. Bioorg. Med. Chem. Lett.* **2010**, *20*, 5139–5142.
S3. H. Kagechika, E. Kawachi, Y. Hashimoto, T. Himi, K. Shudo, *J. Med. Chem.* **1988**, *31*, 2182–2192.
S4. Y. Bekku, *et al. Mol. Cell. Neurosci.* **2003**, *24*, 148–159.
S5. Y. Bekku, *et al. J. Comp. Neurol.* **2012**, *520*, 1721–1736.

Journal of Medicinal Chemistry

Article

pubs.acs.org/jmc

Mechanism of Retinoid X Receptor Partial Agonistic Action of 1-(3,5,5,8,8-Pentamethyl-5,6,7,8-tetrahydro-2-naphthyl)-1*H*-benzotriazole-5-carboxylic Acid and Structural Development To Increase Potency

Fuminori Ohsawa,[†] Shoya Yamada,[†,‡] Nobumasa Yakushiji,[†] Ryosuke Shinozaki,[†] Mariko Nakayama,[†] Kohei Kawata,[†] Manabu Hagaya,[†] Toshiki Kobayashi,[†] Kazutaka Kohara,[†] Yuuki Furusawa,[†] Chisa Fujiwara,[†] Yui Ohta,[†] Makoto Makishima,[§] Hirotaka Naitou,[∥] Akihiro Tai,[⊥] Yutaka Yoshikawa,[#] Hiroyuki Yasui,[#] and Hiroki Kakuta*[,†]

[†]Division of Pharmaceutical Sciences, Okayama University Graduate School of Medicine, Dentistry and Pharmaceutical Sciences, 1-1-1, Tsushima-Naka, Kita-Ku, Okayama 700-8530, Japan

[‡]Research Fellowship Division, Japan Society for the Promotion of Science, Sumitomo-Ichibancho FS Bldg., 8 Ichibancho, Chiyoda-ku, Tokyo 102-8472, Japan

[§]Division of Biochemistry, Department of Biomedical Sciences, Nihon University School of Medicine, 30-1 Oyaguchi-kamicho, Itabashi-ku, Tokyo 173-8610, Japan

[∥]Graduate School of Nutritional and Environmental Sciences, University of Shizuoka, 52-1 Yada, Suruga-ku, Shizuoka 422-8526, Japan

[⊥]Faculty of Life and Environmental Sciences, Prefectural University of Hiroshima, 562 Nanatsuka-Cho, Shobara, Hiroshima 727-0023, Japan

[#]Department of Analytical and Bioinorganic Chemistry, Division of Analytical and Physical Chemistry, Kyoto Pharmaceutical University, 5 Nakauchi-cho, Misasagi, Yamashina-ku, Kyoto 607-8414, Japan

Supporting Information

ABSTRACT: We have reported that retinoid X receptor (RXR) partial agonist 1-(3,5,5,8,8-pentamethyl-5,6,7,8-tetrahydro-2-naphthyl)-1*H*-benzotriazole-5-carboxylic acid (CBt-PMN, **4a**) shows a significant antidiabetes effect in the KK-A^y type 2 diabetes model mice, with reduced side effects compared to RXR full agonists. To elucidate the mechanism of the RXR partial agonist activity of **4a**, we synthesized derivatives of **4a**, evaluated their RXR agonist activity, and performed structure−activity relationship analysis. Reporter gene assay revealed that though **6b**, which possesses an amino group at the 2-position of 5-carboxybenzimidazole, showed RXR full-agonist activity, compounds **6d** and **6e**, which possess an oxygen atom and a sulfur atom at the corresponding position, respectively, showed weak RXR agonist activity. On the other hand, **6c**, which has a trifluoromethyl group at the corresponding position, acts as an RXR partial agonist, having similar E_{max} (67 ± 2%) and lower EC_{50} (15 ± 0 nM) compared to those of **4a** (E_{max} = 75 ± 4%, EC_{50} = 143 ± 2 nM). A fluorescence polarization assay of cofactor recruitment confirmed that fluorescein-labeled D22 coactivator peptide was less efficiently recruited to RXR by **4a** and **6c** than by LGD1069 (**1**), a known RXR full agonist. Electrostatic potential field calculations and computational docking studies suggested that full agonists show an electrostatic attraction, which stabilizes the holo structure and favors coactivator recruitment, between the side chain at the benzimidazole 2-position and the α-carbonyl oxygen of asparagine-306 in helix 4 (H4) of the RXR receptor. However, RXR partial agonists **4a** and **6c** lack this interaction. Like **4a**, **6c** showed a significant antidiabetes effect in KK-A^y type 2 diabetes model mice with reduced levels of the side effects associated with RXR full agonists. These findings should aid the design of new RXR partial agonists as antitype 2 diabetes drug candidates.

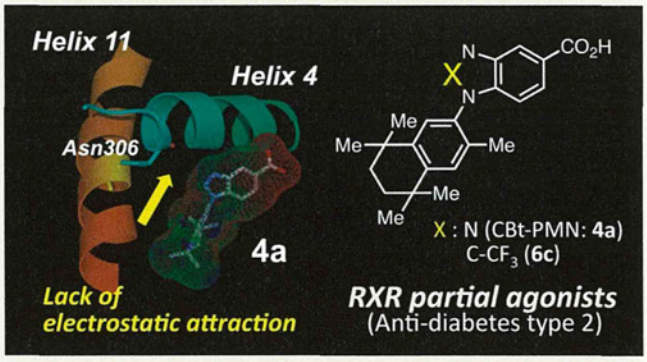

INTRODUCTION

Retinoid X receptors (RXRs) are nuclear receptors that act as ligand-dependent transcription factors and function as the homodimer or as heterodimers with other nuclear receptors, such as retinoic acid receptors (RARs), peroxisome proliferator-activated receptors (PPARs), or liver X receptors (LXRs).[1−3] Interestingly, so-called permissive heterodimers, such as PPAR/RXR[4−6] and

Received: October 3, 2012
Published: February 7, 2013

LXR/RXR,[7−10] which regulate glucose/lipid metabolism and immune response, can be activated by RXR agonists alone.[11] Therefore, RXR agonists are considered to be candidate therapeutic agents for the treatment of type 2 diabetes and autoimmune disease. In addition, synthetic RXR agonists are being used as therapies for other indications. For example, bexarotene (**1**) is approved for treatment of subcutaneous T-cell lymphoma (STCL) in the United States.[12] Although several RXR agonists have been created (Figure 1),[13−17] they were

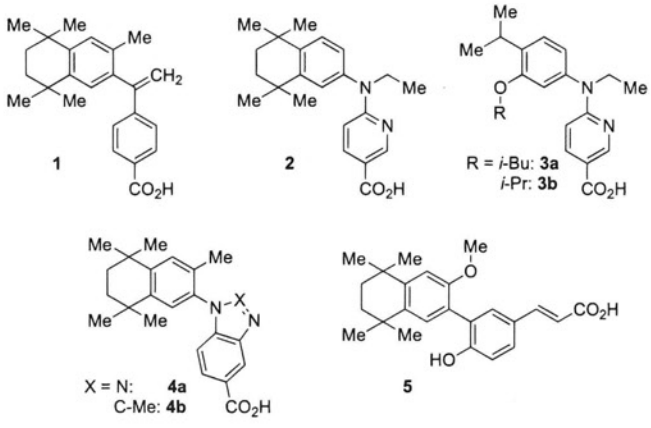

Figure 1. Chemical structures of known RXR ligands **1**−**5**.

found to induce body weight gain,[18] hepatomegaly,[19] blood triglyceride (TG) elevation,[20] and other adverse effects. However, it has been reported that RXR agonists show different patterns of RXR heterodimer activation.[21] Further, when we evaluated the therapeutic and side effects of NEt-TMN (**2**), NEt-3IB (**3a**), and NEt-3IP (**3b**) in KK-A^y type 2 diabetes model mice, we found similar activation of RXR homodimer but different patterns of RXR heterodimer activation.[22] These compounds show therapeutic effects, but also show some of the side effects reported for other RXR agonists.

All RXR agonists that exhibit severe side effects are RXR full agonists, which activate RXR completely. Thus, in our previous work, we hypothesized that there is a difference in RXR activation threshold for the appearance of the therapeutic effects and the side effects. In other words, we considered that RXR partial agonists, whose maximum activation of RXR is lower than that of RXR full agonists, might induce the desired medicinal effects without (or at least with reduced levels of) the side effects that are associated with RXR full agonists. To test this idea, we designed and synthesized RXR partial agonists based on **1** or **2** by linking the acidic domain and the linking domain of **1** or **2**, with the aim of restricting the molecular flexibility. This approach yielded the RXR partial agonist CBt-PMN (**4a**), which indeed showed a significant antidiabetes effect in KK-A^y type 2 diabetes model mice but with reduced levels of the side effects associated with RXR full agonists.[16] However, the reason why **4a** acts as an RXR partial agonist was not established.

In the present work, we aimed to elucidate the mechanism of RXR partial agonistic activity of **4a**, and for this purpose we synthesized a series of derivatives of **4a** for structure−activity relationship analysis. We noted that CBiM-PMN (**4b**),[16] which possesses a methyl group at the benzimidazole 2-position, shows RXR full agonistic activity, and thus we considered that the heterocyclic moiety, especially the 2-position, might be critical for RXR agonistic activity. Therefore, we focused on modification of the heterocyclic ring of **4a** at the 2-position (Figure 2).

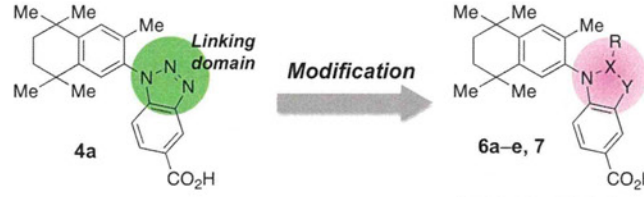

	R-X-Y
6a	H-C=N
6b	NH_2-C=N
6c	CF_3-C=N
6d	O=C-NH
6e	S=C-NH
7	H-C=CH

Figure 2. Molecular design strategy for creating derivatives of **4a**.

Indeed, we found that **6c**, which possesses a trifluoromethyl group at the benzimidazole 2-position, has similar E_{max} and lower EC_{50} values compared to those of **4a**, showing that **6c** is a more potent RXR partial agonist than **4a**. To interpret the structure−activity relationship findings, we carried out electrostatic potential field calculations and computational docking studies. The results indicated that docked RXR full agonists exhibit an electrostatic attraction between the side chain at the benzimidazole 2-position and the α-carbonyl oxygen of asparagine-306 in helix 4 (H4) of the RXR receptor. Such an interaction would serve to stabilize the holo structure, favoring coactivator recruitment. However, RXR partial agonists **4a** and **6c** lack this interaction. We also confirmed that **6c** shows a significant antidiabetes effect in KK-A^y type 2 diabetes model mice with reduced levels of the side effects associated with RXR full agonists.

■ CHEMISTRY

Compounds were synthesized as illustrated in Schemes 1 and 2. Compound **10** was synthesized by nitration and hydrogen reduction from **8**, the synthesis of which has already been reported.[16] On the other hand, compound **13** was obtained from 4-iodobenzoic acid (**11**) by nitration and protection of the carboxyl group as the methyl ester. Compound **14** was synthesized from **10** and **13** by Buchwald coupling reaction, and the common intermediate **15** was obtained from **14** by hydrogen reduction. Compounds **16a**−**e** were synthesized by a ring-closing reaction using formic acid, cyanogen bromide, trifluoroacetic anhydride, triphosgene, and carbon disulfide, respectively. Hydrolysis of the ester group under alkaline conditions afforded the desired products **6a**−**e** (Scheme 1). Compound **7** was obtained by alkaline saponification from **19**, which was synthesized from **17** (obtained as previously reported[23]) and **18** by Ullmann condensation (Scheme 2).

■ RESULTS AND DISCUSSION

The compounds obtained were evaluated by reporter gene assay using COS-1 cells (Table 1). Among the compounds bearing a side chain at the 2-position in the benzimidazole ring, amino derivative **6b** activated RXRα as potently as **2** and **4b**, as previously reported.[16] Compounds **6d** and **6e** showed low efficacy, even at 10 μM. On the other hand, compound **6a**, which has no side chain at the 2-position in the benzimidazole ring, as well as trifluoromethyl derivative **6c** and compound **7**

dx.doi.org/10.1021/jm400033f | J. Med. Chem. 2013, 56, 1865−1877

Scheme 1[a]

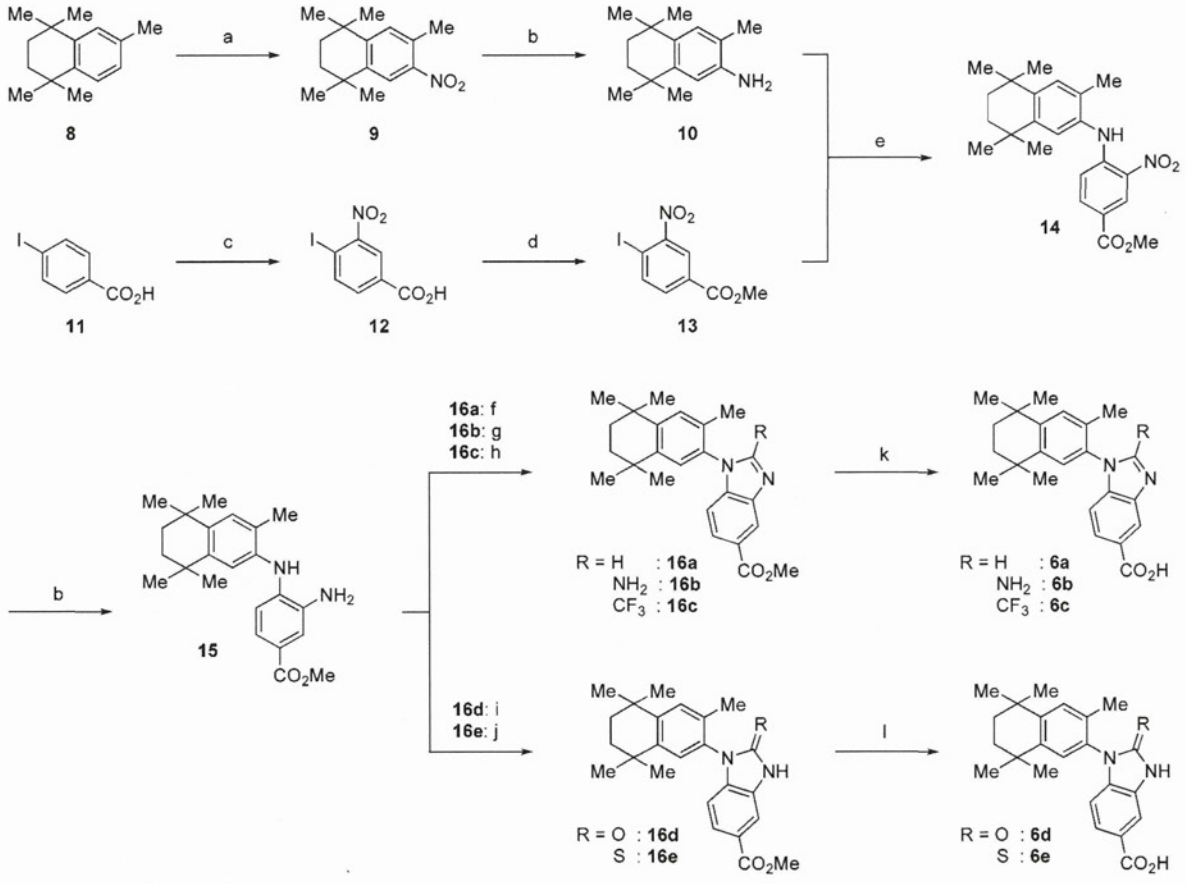

[a](a) HNO_3, Ac_2O, 72%. (b) H_2, Pd–C, EtOAc, 84%–qy. (c) HNO_3, H_2SO_4, 90%. (d) H_2SO_4, MeOH, qy. (e) $Pd_2(dba)_3$, *rac*-BINAP, Cs_2CO_3, toluene, qy. (f) HCO_2H, 93%. (g) BrCN, THF, 26%. (h) TFAA, TFA, 95%. (i) Triphosgene, TEA, DCE, qy. (j) CS_2, DBU, DMF, 93%. (k) (1) 2 N NaOH, MeOH, THF; (2) 2 N HCl, 43%–qy. (1) 2 N NaOH, MeOH; (2) 2 N HCl, 86%–qy.

Scheme 2[a]

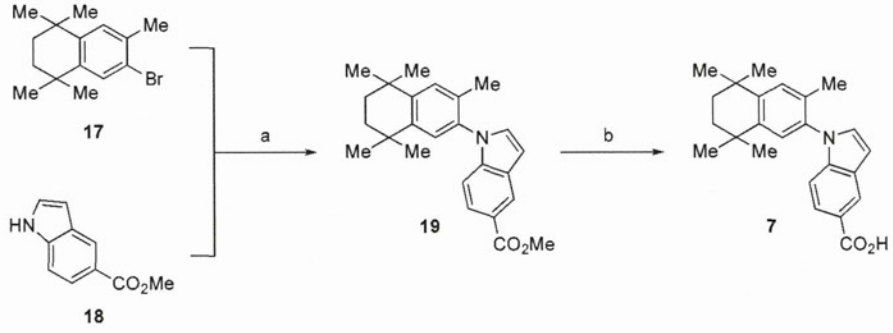

[a](a) CuI, DMEDA, K_3PO_4, toluene, 7.9%. (b) (1) 2 N NaOH, MeOH, THF; (2) 2 N HCl, 92%.

possessing an indole structure, showed lower E_{max} values than those of **2**, **4b**, and **6b**.

According to the review by Pierre Germain et al., nuclear receptor partial agonists are defined as ligands that are potent but exhibit reduced efficacy when compared with full agonists.[24] These compounds can also induce antagonist conformation. For example, PPARγ partial agonist GW0072 is reported to act as a competitive antagonist of rosiglitazone, a PPAR full agonist, despite exhibiting weak PPARγ agonist activity.[25] Thus, to examine whether **6a**, **6c**, and **7** are RXR partial agonists, we evaluated their competitive antagonistic activity against 1 μM **1**. The dose–response curves in the absence of **1** showed that **4a**, **6a**, **6c**, and **7** exhibit RXR agonist activity (Figure 3a). However, since only **4a** and **6c** behaved as competitive antagonists in the presence of **1** (Figure 3b), only these two compounds were considered to be RXR partial agonists.

The ligand-dependent transcription of RXR dimers is induced by conformational change of the receptor from the apo-form (a ligand-free form that recruits a corepressor) to the holo-form (an agonist-binding form that recruits a coactivator).[26] RXR partial agonists are thought to recruit both coactivators and corepressors, acting also as RXR partial antagonists, and it is thought that the recruitment of each type of cofactor by partial agonists is less efficient than that by full

dx.doi.org/10.1021/jm400033f | J. Med. Chem. 2013, 56, 1865–1877

Table 1. Cotransfection Data for 2, 4a, 4b, 6a–e, and 7 towards RXRα in COS-1 Cells and Substituent Constants at the Heterocyclic 2-Position

	efficacy[a,b] (%)					properties of R	
compd	at 0.1 μM	at 1 μM	at 10 μM	EC_{50} (nM)[c]	E_{max} (%)	Es[d]	π[e]
2	86 ± 2	96 ± 4	98 ± 3	3.8 ± 0.2	96 ± 4	–	–
4a	24 ± 2	75 ± 3	69 ± 3	143 ± 2	75 ± 4	–	–
4b	28 ± 1	70 ± 4	80 ± 5	367 ± 130	94 ± 5	−1.24	0.56
6a	NA	52 ± 3	72 ± 4	633 ± 33	75 ± 3	0.00	0.00
6b	NA	35 ± 3	96 ± 4	155 ± 10	103 ± 2	−0.61	−1.23
6c	21 ± 2	65 ± 1	71 ± 6	15 ± 0	67 ± 2	−2.40	0.88
6d	NA	NA	22 ± 2	–	–	–	–
6e	NA	NA	37 ± 0	–	–	–	–
7	45 ± 3	67 ± 5	77 ± 4	83 ± 8	73 ± 2	0.00	0.00

[a]The relative transactivation activity is based on the luciferase activity of 1 μM **1** (RXR full agonist) taken as 100%. All values represent the mean value of at least three separate experiments with triplicate determinations. [b]NA means nonactive (the value is less than 5). [c]EC_{50} values were determined from full dose–response curves. [d]Es: Taft's steric substituent constant (steric effect). [e]π: lipophilicity. These data were cited from Hansch, C.; Leo, A. *Substituent Constants for Correlation Analysis in Chemistry and Biology*; Wiley-Interscience: New York, 1979.

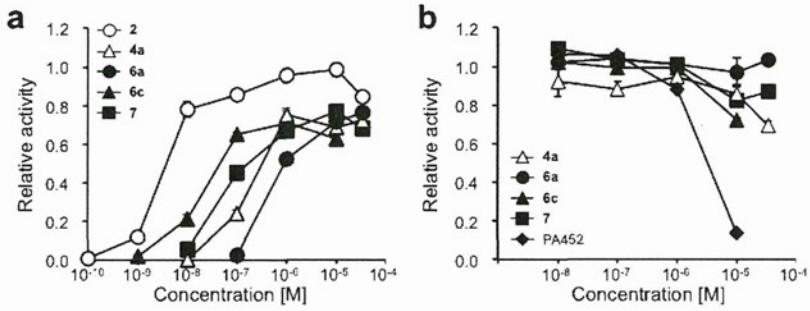

Figure 3. Relative transactivation activities of **2**, **4a**, **6a**, **6c**, and **7** toward RXRα. (a) Dose-dependence of RXRα agonist activities of **2** (open circles), **4a** (open triangles), **6a** (closed circles), **6c** (closed triangles), and **7** (closed squares). (b) Dose-dependence of RXRα antagonist activities of **4a** (open triangles), **6a** (closed circles), **6c** (closed triangles), 7 (closed squares), and PA452 (closed diamond) in the presence of 1 μM **1**. The transactivation activity is shown as relative activity based on the luciferase activity of 1 μM **1** taken as 1.0. Error bars are SEM.

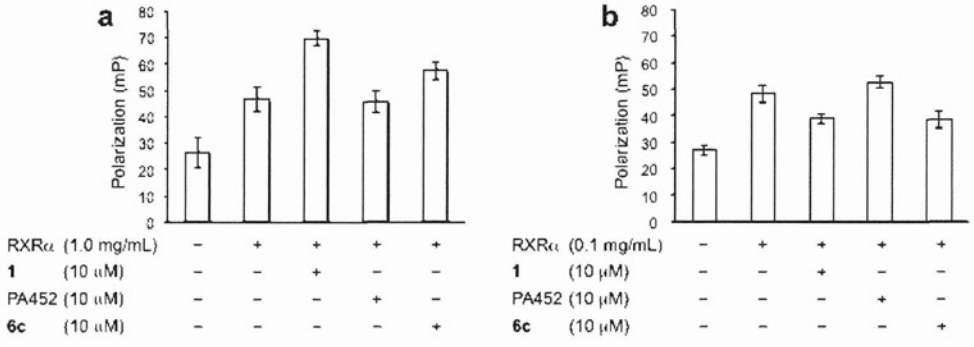

Figure 4. Changes in fluorescence polarization of (a) 5 nM fluorescein-labeled coactivator peptide D22 or (b) 5 nM fluorescein-labeled corepressor peptide SMRT-ID2 induced by **6c** (putative partial agonist), compound **1** (RXR full agonist), and PA452 (RXR antagonist). Fluorescence polarization values, expressed in mP, are the mean ± SEM of measurements obtained from triplicate wells.

agonists or full antagonists. Thus, we examined cofactor recruitment by our putative RXR partial agonists. Cofactor recruitment assay was performed using fluorescence polarization measurements with RXR receptor, each ligand and fluorescein-labeled cofactors according to Lévy-Bimbot et al.[27,28] If a fluorescein-labeled cofactor does not bind to the receptor, the degree of fluorescence polarization (FP) will be low, because the fluorescein-labeled cofactor retains high mobility. However, binding of the cofactor to the receptor reduces the mobility and induces a high FP value. Thus, addition of an agonist to a mixture of fluorescein-labeled coactivator and RXR receptor should result in a higher FP value than that in its absence.

As coactivator and corepressor peptides, we selected D22[29] and silencing mediator for retinoid and thyroid hormone receptors interaction domain 2 (SMRT-ID2),[30] respectively. D22 has been used for time-resolved fluorescence resonance energy transfer (TR-FRET) assay with RXR.[29] SMRT-ID2 is reported to bind to apo-RXR.[30] First, to determine the appropriate RXR concentration for this assay, we evaluated FP values at various RXR concentrations with each fluorescein-labeled cofactor (5 nM) in the absence or presence of **1** (1 μM). As the

dx.doi.org/10.1021/jm400033f | J. Med. Chem. 2013, 56, 1865–1877

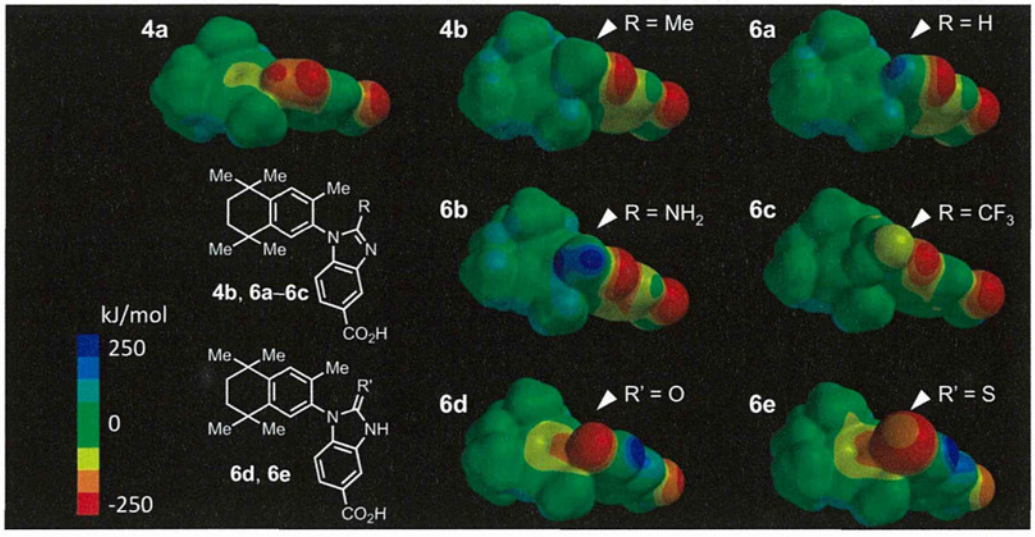

Figure 5. Calculated electrostatic potential distribution of **4a**, **4b**, and **6a–e**.

RXR concentration was increased, the FP value also increased, indicating the binding of each peptide with RXR (Supporting Information, Figure S1). In the presence of full agonist **1**, the plot for fluorescein-labeled D22 was shifted to the left, indicating that **1** induced interaction of D22 with RXR. On the other hand, the plot for fluorescein-labeled SMRT-ID2 was shifted to the right in the presence of **1**, indicating that **1** decreased the interaction between SMRT-ID2 and RXR. The RXR concentration showing the largest change of FP by **1** was 1.0 mg/mL for fluorescein-labeled D22 or 0.1 mg/mL for SMRT-ID2, and therefore these RXR concentrations were used in subsequent experiments. Using these conditions, we compared the cofactor recruitment ability of RXR partial agonists **4a** and **6c** with those of RXR full agonist **1** and RXR antagonist PA452.[31] Each compound was used at 10 μM, because we found no difference in recruitment of fluorescein-labeled D22 between 10 and 33 μM concentrations (Supporting Information, Figure S2). As shown in Figures S2 (Supporting Information) and 4, the coactivator recruitment ability of both RXR partial agonists was intermediate between those of RXR full agonist **1** and RXR antagonist PA452. On the other hand, the corepressor recruitment ability of RXR partial agonist **6c** was less than that of PA452 and similar to that of RXR full agonist **1**. Taken together with the results of reporter gene assay and cofactor recruitment assay, these findings confirm that **6c** is a RXR partial agonist, like **4a**.

To examine the effects of substituents at the benzimidazole 2-position, we performed structure–activity relationship analysis of **2**, **4a**, **4b**, and **6a–c** (Table 1). Considering their Taft's steric substituent constants (Es) and lipophilicity (π), we found that these two constants appeared not to be related to RXR agonistic activity, indicating that electronic properties at the benzimidazole 2-position are critical for RXR agonistic activity.

Thus, to investigate the spatial electronic properties of these compounds, we calculated the electrostatic potential field using Spartan 10 (Figure 5). The RXR full agonists **4b** and **6b** have a positive electrostatic potential field at the benzimidazole 2-position, while RXR partial agonist **6c** has a weak negative electrostatic potential field at that position. On the other hand, **6d** and **6e**, which showed weak RXR agonistic activity, have a stronger negative electrostatic potential field at the benzimidazole 2-position than **6c**. These results suggest that a positive electrostatic potential field at the benzimidazole 2-position, as in **4b** and **6b**, is important to stabilize the holo structure, thereby favoring coactivator recruitment for RXR full agonistic activity.

Next, to examine the interaction between the electrostatic potential field around the heterocyclic 2-position and RXRα, we performed a docking study using AutoDock 4.2[32] (Figure 6 and Table 2). The results reveal that the 2-position of the heterocyclic ring in **4a**, **4b**, **6b**, and **6c** is close to the α-carbonyl oxygen of asparagine-306 (Asn306) in helix 4 (H4; jade green). Thus, full agonists **4b** and **6b**, which have a positive electrostatic potential field at the 2-position of the heterocyclic ring, may have an attractive interaction with Asn306 in H4. In turn, this interaction may promote the proper folding of helix 12 (H12; red), stabilizing the holo form and thus favoring recruitment of a coactivator. On the other hand, **6d** and **6e**, which have a strong negative electrostatic potential field at the

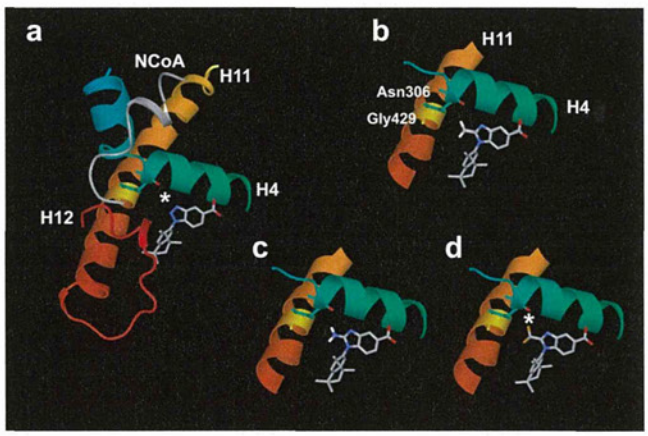

Figure 6. (a) Docking model of RXR partial agonist **4a** in the ligand-binding pocket of RXRα (PDB code 3H0A). H4, H11, and H12 mean helix 4 (jade green), helix 11 (orange), and helix 12 (red), respectively. (b) Docking model of RXR full agonist **4b** in the ligand-binding pocket of RXRα. (c) Docking model of RXR full agonist **6b** in the ligand-binding pocket of RXRα. (d) Docking model of RXR partial agonist **6c** in the ligand-binding pocket of RXRα. The asterisk indicates electrostatic repulsion.

dx.doi.org/10.1021/jm400033f | J. Med. Chem. 2013, 56, 1865–1877

Table 2. Docking Score and Distance between the α-Carbonyl Oxygen of Asn306 and the Closest Atom at the Heterocyclic 2-Position of Each Compound

compd	docking score	mean binding energy (kcal/mol)	distance (Å)	atom
2	–	–	–	–
4a	100/100	−11.92	4.42	N
4b	100/100	−12.13	2.67	H
6a	100/100	−11.45	3.85	H
6b	100/100	−11.72	2.66	H
6c	100/100	−11.41	2.51	F
6d	100/100	−11.49	3.88	O
6e	100/100	−11.97	3.39	S
7	100/100	−11.67	3.88	H

2-position of the heterocyclic ring, would exhibit electrostatic repulsion between the 2-position of the heterocyclic ring and Asn306. Such electrostatic repulsion may reduce the affinity for RXR and lead to a steric clash between Asn306 in H4 and glycine-429 (Gly429) in helix 11 (H11; orange), thereby unstabilizing the holo form. On the other hand, compounds **4a** and **6c** lack the electrostatic attractive force because these compounds possess a weak negative electrostatic field around the 2-position of the heterocyclic ring. Thus, RXR partial agonists might be less able to induce stable folding of H12 in RXR for coactivator recruitment, as compared to RXR full agonists. These results suggest that the nature of the interaction between a ligand and H4 is important for determining whether the ligand exerts RXR full agonistic or partial agonistic activity.

We found that **6c** is a more potent RXR partial agonist than **4a**. Thus, we next examined the activities of **6c** toward other RXR subtypes, as well as RARs, PPARγ, LXRα, PPARγ/RXRα, and LXRα/RXRα, by means of reporter gene assay. Compound **6c** showed partial agonistic activities toward RXRβ and RXRγ, but caused little activation of RARs (Supporting Information, Figure S3). In addition, **6c** showed no PPARγ agonistic activity but activated LXRα, LXRα/RXRα, and PPARγ/RXRα (Supporting Information, Figure S4). Compounds **4a** and **6c** also showed RXR partial agonist activity toward mouse RXRα (Supporting Information, Figure S5), as well as human RXRα. Thus, **6c** can be expected to show antidiabetic effects in mice, similar to **4a**.

Since **6c** shows similar receptor activation patterns to **4a**,[16] we were interested in the anti-type 2 diabetes effect and the side effects of **6c**. First, we confirmed that single oral administration of **6c** at 30 mg/kg resulted in a blood concentration over 6 μM in ICR male mice (Supporting Information, Figure S6). Then, to evaluate side effects associated with RXR full agonists, changes in body weight, hepatomegaly, blood triglyceride (TG), and blood total cholesterol (TCHO) were assessed when **6c**, RXR full agonist **2**, and **4b** were administered orally to ICR mice at 30 mg/kg/day for 7 days (Figure 7). Despite developing slight hepatomegaly, the group treated with **6c** showed a similar body weight gain to the control group and did not show blood TG or TCHO elevation, whereas the group treated with **2** or **4b** showed significant increases of body weight gain and blood TG level compared with the control. We found no significant differences of renal function parameters between the treated and the vehicle control groups (Supporting Information, Table S2). Since liver function parameters (in particular, alkaline phosphatase, ALP) were elevated, the hepatomegaly may be associated with hepatotoxicity related to the chemical

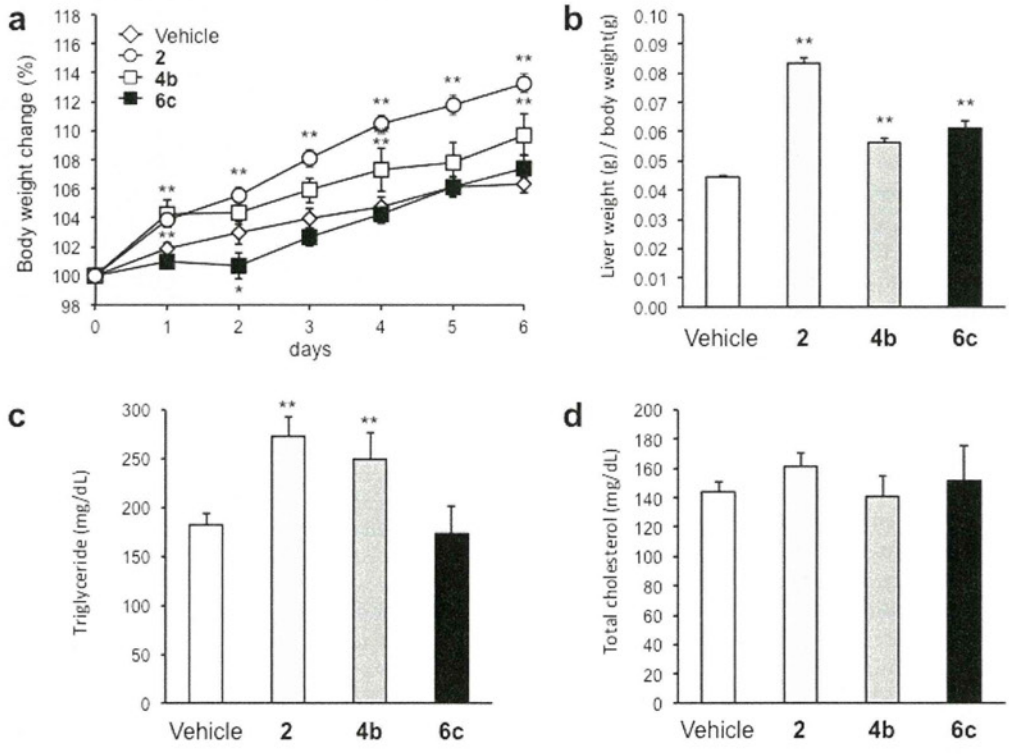

Figure 7. Evaluation of adverse effects of repeated oral administration of compounds at 30 mg/kg/day to male ICR mice for 7 consecutive days. (a) Time course of body weight change. Diamond, circles, open squares, and closed squares indicate vehicle, **2**, **4b**, and **6c**, respectively. Effects of compounds on (b) liver weight gain, (c) serum triglyceride, and (d) total cholesterol, respectively. The data (n = 7–23) represent the mean ± SEM. Statistical analysis was performed by analysis of variance (ANOVA). Significant difference: *p < 0.05 vs vehicle. **p < 0.01 vs vehicle.

dx.doi.org/10.1021/jm400033f | J. Med. Chem. 2013, 56, 1865–1877

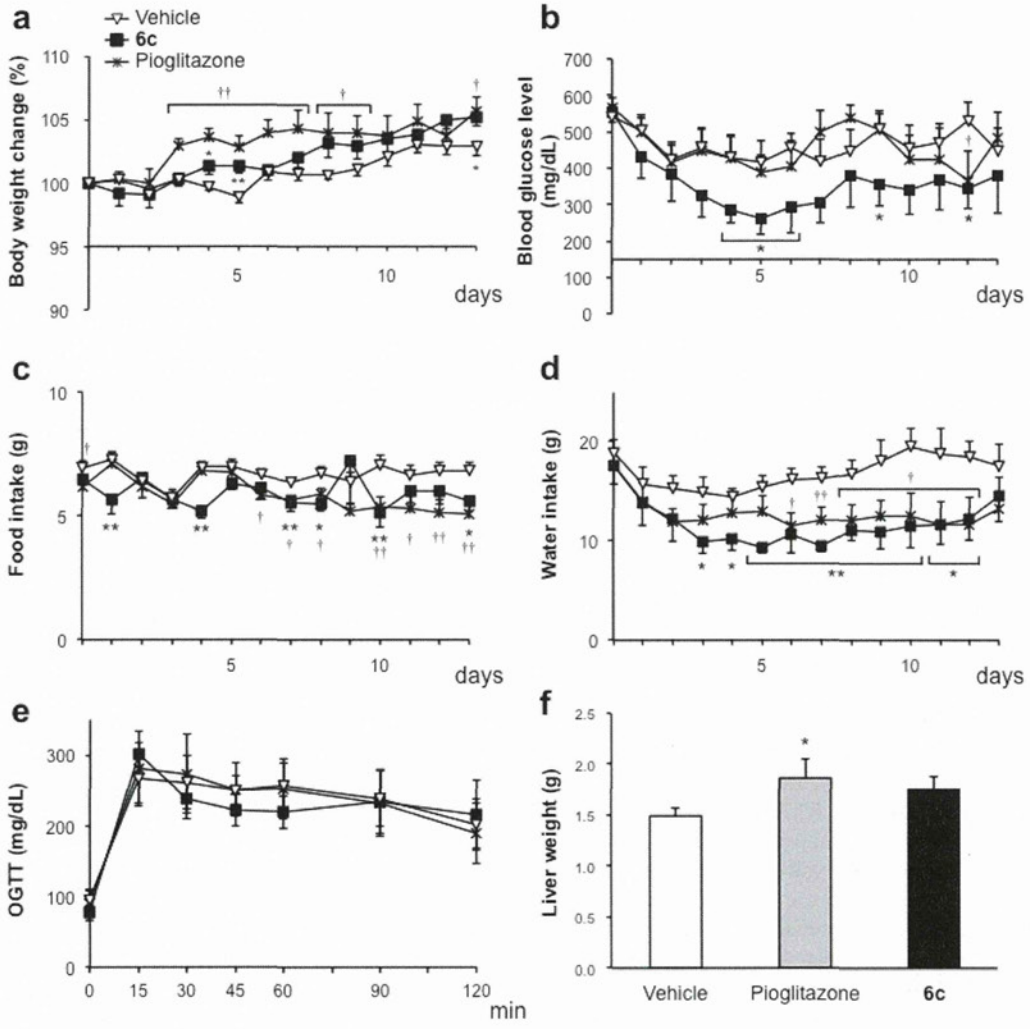

Figure 8. Evaluation of anti-type 2 diabetes effects of repeated oral administration of **6c** or pioglitazone at 10 mg/kg/day to male KK-A^y mice for 14 consecutive days. Time course of (a) body weight change, (b) blood glucose levels. (c) food intake, (d) water intake, and (e) oral glucose tolerance test (OGTT) results. (f) Liver weight gain in male KK-A^y mice treated with vehicle and compounds. Inverted triangles, closed squares, and asterisks indicate vehicle, **6c**, and pioglitazone, respectively. The data (n = 4–5) represent the mean ± SEM. Statistical analysis was performed by analysis of variance (ANOVA). Significant difference: *p < 0.05, **6c** vs vehicle. **p < 0.01, **6c** vs vehicle. †p < 0.05, pioglitazone vs vehicle. ††p < 0.01, pioglitazone vs vehicle.

structure of **6c**. Nevertheless, the hepatomegaly induced by **6c** is clearly less marked than that induced by RXR full agonist **2**.

Further, when **6c** was administered orally to male and female SD rats at 30 mg/kg/day for 28 days, we observed hepatotoxicity similar to that in the case of administration to ICR mice for 7 days, together with slight enlargement of the spleen, but there was no significant difference in body weight change or in the weights of other organs (Supporting Information, Figure S7 and Tables S3 and S4). As for blood constituents, some significant differences from the vehicle were observed, but the data, other than liver function parameters, were all within the ranges considered normal by the suppliers.

Next, we examined the antitype 2 diabetes activity in KK-A^y mice. Compound **6c** or pioglitazone was orally administered at 10 mg/kg/day for 14 days (Figure 8). The group treated with **6c** did not show significant improvement in the oral glucose tolerance test (OGTT) compared to the control group (Figure 8e), but the average blood glucose level in the group treated with **6c** was significantly reduced at days 4–6, 9, and 12 (Figure 8b). Compound **6c** also reduced water intake significantly at days 3–12 compared to vehicle-treated mice (Figure 8d), thus showing significant anti-type 2 diabetes effects.

Table 3. Plasma Parameters of Male KK-A^y Mice after Oral Administration of Vehicle, 6c, or Pioglitazone at 10 mg/kg/day for 14 Consecutive Days[a]

	vehicle	pioglitazone	6c
AST (U/l)	49.6 ± 2.3	45.3 ± 8.4	42.3 ± 2.9
ALT (U/l)	17.6 ± 0.9	21.3 ± 1.9*	17.3 ± 2.6
γ-GTP (U/l)	5.8 ± 0.6	7.3 ± 2.3	6.3 ± 0.3
ALP (U/l)	358.2 ± 43.1	395.7 ± 44.1	554.0 ± 113.2*
CRE (mg/dL)	DL	DL	DL
BUN (mg/dL)	21.9 ± 1.1	22.2 ± 1.3	22.5 ± 1.1
TG (mg/dL)	122.4 ± 11.0	124.0 ± 28.5	185.0 ± 38.0
TCHO (mg/dL)	153.2 ± 11.1	147.3 ± 3.8	155.3 ± 10.7

[a]The data (n = 3–5) represent the mean ± SEM. Statistical analysis was performed by analysis of variance (ANOVA). Significant difference: *p < 0.05 vs vehicle. **p < 0.01 vs vehicle. DL means detection limit (0.2 mg/dL).

dx.doi.org/10.1021/jm400033f | J. Med. Chem. 2013, 56, 1865–1877

These effects also may result partially or entirely from activation of PPAR/RXR or LXR/RXR activation by **6c**. Moreover, **6c** did not elevate blood TG or blood TCHO significantly (Table 3). These results support our hypothesis of a threshold difference for the therapeutic and side effects of RXR agonists and indicate that RXR partial agonists represent a promising class of candidate anti-type 2 diabetes agents with reduced levels of the serious adverse effects caused by RXR full agonists.

CONCLUSION

In order to elucidate the mechanism of action of the RXR partial agonist **4a**, we synthesized several derivatives of **4a** and performed structure−activity relationship analysis. The results of electrostatic potential field calculations and computational docking studies indicated that the electrostatic attraction between an oxygen atom of Asn306 in H4 and the 2-position at the benzimidazole ring, which is observed in RXR full agonists, is absent in the partial agonists **4a** (reported previously) and **6c** (newly synthesized in this work). The presence of this interaction would stabilize the holo form of RXR and favor coactivator recruitment. Compound **6c** showed similar E_{max} and lower EC_{50} values toward RXR compared to **4a**. Fluorescence polarization assay of cofactor recruitment confirmed its partial agonist character. We evaluated its side effects in ICR mice and SD rats, as well as its therapeutic effects in the KK-A^y mouse model of type 2 diabetes. Although **6c** induced slight hepatomegaly, the degree of hepatomegaly was less than that induced by RXR full agonists **2** and **4b**. We confirmed that **6c** had a significant antidiabetes effect in KK-A^y type 2 diabetes model mice with less side effects than RXR full agonists. These results indicate that RXR partial agonists are promising candidates for antidiabetes drugs with reduced levels of the side effects associated with full agonists. Further structural modification of our compounds may generate attractive candidates for antitype 2 diabetes agents.

EXPERIMENTAL SECTION

Chemistry. *General.* Melting points were determined with a Yanagimoto hot-stage melting point apparatus and are uncorrected. IR spectra were recorded on a JASCO FT/IR350 (KBr). ^{1}H NMR spectra were recorded on a JEOL JNM-AL300 FT-NMR system (300 MHz), a Varian VXR-300 (300 MHz) spectrometer, or a Varian VXR-500 (500 MHz) spectrometer. FAB-MS was carried out with a VG70-SE. The purity of all tested compounds was >95%, as confirmed by combustion analysis or by HPLC analysis. Elemental analysis was carried out with a Yanagimoto MT-5 CHN recorder elemental analyzer, and results were within ±0.4% of the theoretical values. The HPLC system used in this study was a Shimadzu liquid chromatographic system (Kyoto, Japan) consisting of an LC-10AD pump, SPD-10AV UV−vis spectrophotometric detector, CTO-10AS column oven and C-R5A Chromatopac. The samples (each 20 μL) were injected and the chromatographic analyses were carried out on an Inertsil ODS-3 (4.6 i.d. × 250 mm, 5 μm, GL Sciences, Tokyo, Japan) with a guard column of Inertsil ODS-3 (4.0 i.d. × 10 mm, 5 μm, GL Sciences) at 40 °C, using methanol:16.7−50 mM ammonium acetate (final concentration at 5 mM) (adjusted with acetic acid to pH 5.0) (90:10, 80:20, or 70:30, v/v) as a mobile phase. The flow rate was 0.7 mL/min and the absorbance at 280 nm was monitored.

*4-[1-(3,5,5,8,8-Pentamethyl-5,6,7,8-tetrahydronaphthalen-2-yl)-ethenyl]benzoic Acid (**1**).* This compound was prepared according to ref 13. HPLC: 11.6 min; >95% purity (MeOH:$AcONH_4$(aq) = 90:10).

*6-[Ethyl(5,5,8,8-tetramethyl-5,6,7,8-tetrahydronaphthalen-2-yl)-amino]nicotinic Acid (**2**).* This compound was prepared according to ref 14. HPLC: 24.9 min; >95% purity (MeOH:$AcONH_4$(aq) = 80:20).

*1-(3,5,5,8,8-Pentamethyl-5,6,7,8-tetrahydro-2-naphthyl)-1H-benzotriazole-5-carboxylic Acid (**4a**).* This compound was prepared according to ref 16. HPLC: 13.8 min; >95% purity (MeOH:$AcONH_4$(aq) = 80:20).

*2-Methyl-1-(3,5,5,8,8-pentamethyl-5,6,7,8-tetrahydro-2-naphthyl)-1H-benzoimidazole-5-carboxylic Acid (**4b**).* This compound was prepared according to ref 16. HPLC: 14.0 min; >95% purity (MeOH:$AcONH_4$(aq) = 80:20).

*1,1,4,4,6-Pentamethyl-7-nitro-1,2,3,4-tetrahydronaphthalene (**9**).* To an ice-cooled solution of **8** (2.0 g, 9.9 mmol) in Ac_2O (10 mL) was added dropwise concd HNO_3 (0.75 mL). The reaction mixture was poured into ice and extracted with EtOAc (2 × 50 mL). The organic layer was washed with H_2O (2 × 50 mL) and brine (50 mL), dried over $MgSO_4$, and evaporated under reduced pressure. The residue was recrystallized from EtOAc/hexane to yield 4.5 g of **9** as a pale yellow powder (72%). ^{1}H NMR (300 MHz, $CDCl_3$) δ: 7.96 (s, 1H), 7.21 (s, 1H), 2.56 (s, 3H), 1.70 (s, 4H), 1.30 (s, 6H), 1.29 (s, 6H).

*3,5,5,8,8-Pentamethyl-5,6,7,8-tetrahydronaphthalen-2-ylamine (**10**).* To a solution of **9** (2.5 g, 10 mmol) in EtOAc (20 mL) was added Pd/C (catalytic amount). The mixture was stirred at room temperature (rt) under a H_2 atmosphere for 7.0 h, filtered through Celite, and evaporated under reduced pressure to yield 2.2 g of **10** as a pale yellow solid (qy). ^{1}H NMR (300 MHz, $CDCl_3$) δ: 6.97 (s, 1H), 6.61 (s, 1H), 3.45 (br s, 2H), 2.14 (s, 3H), 1.64 (s, 4H), 1.24 (s, 6H), 1.24 (s, 6H).

*4-Iodo-3-nitrobenzoic Acid (**12**).* To a solution of **11** (2.5 g, 10 mmol) in concd H_2SO_4 (14 mL) was added dropwise a solution of concd HNO_3 (4.9 mL) and concd H_2SO_4 (4.3 mL). The reaction mixture was stirred at rt overnight, poured onto ice (50 mL), and filtered. The filtrate was evaporated, and the residue was dried to yield 2.6 g of **12** as a pale yellow powder (90%). ^{1}H NMR (500 MHz, $CDCl_3$) δ: 8.49 (s, 1H), 8.19 (d, J = 8.0 Hz, 1H), 7.92 (d, J = 8.0 Hz, 2H).

*4-Iodo-3-nitrobenzoic Acid Methyl Ester (**13**).* To a solution of **12** (2.6 g, 9.0 mmol) in dry MeOH (10 mL) was added dropwise concd H_2SO_4 (1.9 mL). The reaction mixture was stirred at rt overnight, neutralized with sat. $NaHCO_3$ (10 mL), and extracted with EtOAc (3 × 40 mL). The organic layer was washed with H_2O (40 mL) and brine (50 mL), dried over $MgSO_4$, and evaporated under reduced pressure. The residue was recrystallized from MeOH to yield 2.8 g of **13** as yellow needles (qy). ^{1}H NMR (500 MHz, $CDCl_3$) δ: 8.45 (d, J = 2.0 Hz, 1H), 8.15 (d, J = 8.0 Hz, 1H), 7.88 (dd, J = 8.0, 2.0 Hz, 1H), 3.97 (s, 3H).

*3-Nitro-4-(3,5,5,8,8-pentamethyl-5,6,7,8-tetrahydronaphthalen-2-ylamino)benzoic Acid Methyl Ester (**14**).* To a solution of **10** (0.83 g, 3.8 mmol) and **13** (1.2 g, 3.8 mmol) in dry toluene (4.0 mL) were added $Pd_2(dba)_3$ (170 mg, 0.19 mmol), *rac*-BINAP (180 mg, 0.28 mmol), and Cs_2CO_3 (3.1 g, 9.5 mmol). The reaction mixture was refluxed at 110 °C under an Ar atmosphere overnight and filtered through Celite. The filtrate was evaporated under reduced pressure. The residue was purified by flash column chromatography (EtOAc:*n*-hexane = 1:15) to yield 1.3 g of **14** as a yellow foam (qy). ^{1}H NMR (300 MHz, $CDCl_3$) δ: 9.63 (br s, 1H), 8.93 (d, J = 2.0 Hz, 1H), 7.93 (dd, J = 9.0, 2.0 Hz, 1H), 7.24 (s, 1H), 7.17 (s, 1H), 6.82 (d, J = 9.0 Hz, 1H), 3.91 (s, 3H), 2.19 (s, 3H), 1.70 (s, 4H), 1.31 (s, 6H), 1.25 (s, 6H).

*3-Amino-4-(3,5,5,8,8-pentamethyl-5,6,7,8-tetrahydronaphthalen-2-ylamino)benzoic Acid Methyl Ester (**15**).* To a solution of **14** (0.50 g, 1.3 mmol) in EtOAc (2.0 mL) was added Pd/C (catalytic amount). The mixture was stirred at rt under a H_2 atmosphere overnight and then filtered through Celite. The filtrate was evaporated under reduced pressure to yield 0.39 g of **15** as a white solid (84%). ^{1}H NMR (300 MHz, $CDCl_3$) δ: 7.49 (s, 1H), 7.48 (d, J = 8.0 Hz, 1H), 7.13 (s, 1H), 6.96 (s, 1H), 6.83 (d, J = 8.0 Hz, 1H), 5.39 (br s, 1H), 3.87 (s, 3H), 3.55 (br s, 2H), 2.19 (s, 3H), 1.67 (s, 4H), 1.28 (s, 6H), 1.21 (s, 6H).

*1-(3,5,5,8,8-Pentamethyl-5,6,7,8-tetrahydronaphthalen-2-yl)-1H-benzoimidazole-5-carboxylic Acid Methyl Ester (**16a**).* To compound **15** (150 mg, 0.40 mmol) was added formic acid (1.0 mL). The reaction mixture was refluxed at 100 °C for 4.0 h, poured into 2 N NaOH (10 mL), and extracted with EtOAc (3 × 40 mL). The organic layer was collected, washed with brine (10 mL), and dried over $MgSO_4$. The solvent was evaporated under reduced pressure.

The residue was purified by flash column chromatography (EtOAc:*n*-hexane = 1:4) to yield 140 mg of **16a** as a colorless powder (93%). ^{1}H NMR (300 MHz, $CDCl_3$) δ: 8.61 (d, J = 2.0 Hz, 1H), 8.06 (s, 1H), 8.03 (dd, J = 9.0, 2.0 Hz, 1H), 7.33 (s, 1H), 7.22 (s, 1H), 7.21 (d, J = 9.0 Hz, 1H), 3.98 (s, 3H), 2.05 (s, 3H), 1.75 (s, 4H), 1.36 (s, 6H), 1.29 (s, 6H).

*2-Amino-1-(3,5,5,8,8-pentamethyl-5,6,7,8-tetrahydronaphthalen-2-yl)-1H-benzoimidazole-5-carboxylic Acid Methyl Ester (**16b**).* To a solution of BrCN (48 mg, 0.45 mmol) in THF (5.0 mL) was added **15** (110 mg, 0.30 mmol). The reaction mixture was stirred at rt under an Ar atmosphere for 12 h, poured into 2 N NaOH (10 mL), and extracted with EtOAc (3 × 60 mL). The organic layer was washed with brine (20 mL) and H_2O (40 mL), dried over $MgSO_4$, and evaporated under reduced pressure. The residue was purified by flash column chromatography (CH_2Cl_2:MeOH = 50:1) to yield 30 mg of **16b** as a white powder (26%). ^{1}H NMR (300 MHz, $CDCl_3$) δ: 8.14 (d, J = 1.5 Hz, 1H), 7.77 (dd, J = 8.5, 1.5 Hz, 1H), 7.34 (s, 1H), 7.23 (s, 1H), 6.81 (d, J = 8.5 Hz, 1H), 3.92 (s, 3H), 2.03 (s, 3H), 1.74 (s, 4H), 1.36 (s, 3H), 1.34 (s, 3H), 1.28 (s, 3H), 1.27 (s, 3H).

*1-(3,5,5,8,8-Pentamethyl-5,6,7,8-tetrahydronaphthalen-2-yl)-2-trifluoromethyl-1H-benzoimidazole-5-carboxylic Acid Methyl Ester (**16c**).* To a solution of **15** (520 mg, 1.4 mmol) in TFA (8.0 mL) was added trifluoroacetic anhydride (1.0 mL, 7.0 mmol). The reaction mixture was stirred at rt for 1.0 h, poured into sat. $NaHCO_3$ (30 mL), and extracted with EtOAc (3 × 50 mL). The organic layer was washed with H_2O (50 mL) and brine (10 mL), dried over $MgSO_4$, and evaporated under reduced pressure. The residue was purified by flash column chromatography (EtOAc:*n*-hexane = 1:20) to yield 590 mg of **16c** as a white solid (95%). ^{1}H NMR (300 MHz, $CDCl_3$) δ: 8.68 (d, J = 1.5 Hz, 1H), 8.10 (dd, J = 9.0, 1.5 Hz, 1H), 7.28 (d, J = 8.5 Hz, 1H), 7.20 (s, 1H), 7.12 (dd, J = 9.0, 0.5 Hz, 1H), 3.97 (s, 3H), 1.89 (s, 3H), 1.73 (s, 4H), 1.35 (s, 6H), 1.25 (s, 6H).

*2-Oxo-1-(3,5,5,8,8-pentamethyl-5,6,7,8-tetrahydro-2-naphthyl)-2,3-dihydro-1H-benzoimidazole-5-carboxylic Acid Methyl Ester (**16d**).* To a solution of **15** (110 mg, 0.30 mmol) in 1,2-dichloroethane (6.0 mL) were added Et_3N (70 μL, 0.50 mmol) and triphosgene (59 mg, 0.20 mmol). The mixture was refluxed at 110 °C overnight, poured into H_2O (40 mL), and extracted with EtOAc (2 × 30 mL). The organic layer was washed with H_2O (60 mL), dried over $MgSO_4$, and evaporated under reduced pressure to yield 120 mg of **16d** as a pale yellow solid (qy). ^{1}H NMR (500 MHz, $CDCl_3$) δ: 11.35 (s, 1H), 7.67 (dd, J = 8.0, 1.5 Hz, 1H), 7.60 (d, J = 1.5 Hz, 1H), 7.39 (s, 1H), 7.27 (s, 1H), 6.66 (d, J = 8.0 Hz, 1H), 3.84 (s, 3H), 2.00 (s, 3H), 1.68 (s, 4H), 1.31 (s, 3H), 1.30 (s, 3H), 1.23 (s, 3H), 1.23 (s, 3H).

*1-(3,5,5,8,8-Pentamethyl-5,6,7,8-tetrahydro-2-naphthyl)-2-thioxo-2,3-dihydro-1H-benzoimidazole-5-carboxylic Acid Methyl Ester (**16e**).* To a solution of **15** (62 mg, 0.17 mmol) in DMF (2.0 mL) were added CS_2 (100 μL, 1.7 mmol) and DBU (25 μL, 0.17 mmol). The reaction mixture was stirred at 50 °C for 0.5 h, poured into H_2O (60 mL), and extracted with EtOAc (3 × 40 mL). The organic layer was washed with H_2O (3 × 80 mL) and brine (80 mL), dried over $MgSO_4$, and evaporated under reduced pressure. The residue was purified by flash column chromatography (EtOAc:*n*-hexane = 1:5) to yield 64 mg of **16d** as a white solid (93%). ^{1}H NMR (300 MHz, $CDCl_3$) δ: 12.3 (br s, 1H), 8.00 (s, 1H), 7.89 (dd, J = 8.5, 1.5 Hz, 1H), 7.34 (s, 1H), 7.22 (s, 1H), 6.81 (d, J = 8.5 Hz, 1H), 3.92 (s, 3H), 2.08 (s, 3H), 1.74 (s, 4H), 1.36 (s, 3H), 1.35 (s, 3H), 1.31 (s, 3H), 1.26 (s, 3H).

*1-(3,5,5,8,8-Pentamethyl-5,6,7,8-tetrahydronaphthalen-2-yl)-1H-benzoimidazole-5-carboxylic Acid (**6a**).* To a solution of **16a** (140 mg, 0.40 mmol) in MeOH (3.0 mL) and THF (1.0 mL) was added 2 N NaOH (2.0 mL). The reaction mixture was stirred at 60 °C for 2.0 h, poured into 2 N HCl (2.0 mL), and extracted with EtOAc (3 × 40 mL). The organic layer was collected, washed with brine (20 mL), dried over $MgSO_4$, and evaporated under reduced pressure to yield 180 mg of **6a** (qy). The residue was recrystallized from EtOAc/*n*-hexane to yield 110 mg of colorless powder. Mp: 255.0–257.0 °C. HPLC: 13 min; 99% purity (MeOH:$AcONH_4$(aq) = 70:30). ^{1}H NMR (300 MHz, $CDCl_3$) δ: 8.76 (d, J = 2.0 Hz, 1H), 8.17 (s, 1H), 8.11 (dd, J = 8.0, 2.0 Hz, 1H), 7.33 (s, 1H), 7.27 (d, J = 8.0 Hz, 1H), 7.26 (s, 1H), 7.23 (s, 1H), 2.06 (s, 3H), 1.74 (s, 4H), 1.36 (s, 6H), 1.29 (s, 6H). FAB-MS m/z: 363 $[M + H]^+$.

*2-Amino-1-(3,5,5,8,8-pentamethyl-5,6,7,8-tetrahydronaphthalen-2-yl)-1H-benzoimidazole-5-carboxylic Acid (**6b**).* To a solution of **16b** (95 mg, 0.24 mmol) in MeOH (2.0 mL) and THF (2.0 mL) was added 2 N NaOH (2.0 mL). The reaction mixture was stirred at 60 °C for 0.5 h, poured into 2 N HCl (4.0 mL), and extracted with EtOAc (3 × 70 mL). The organic layer was collected, washed with brine (30 mL) and H_2O (30 mL), dried over $MgSO_4$, and evaporated under reduced pressure. The residue was purified by flash column chromatography (CH_2Cl_2:MeOH = 10:1) to yield 110 mg of **6b** as white crystals (qy). Mp: 226.2–227.9 °C. HPLC: 25 min; >95% purity (MeOH:$AcONH_4$(aq) = 70:30). ^{1}H NMR (300 MHz, DMSO-d_6) δ: 12.95 (br s, 1H), 8.36 (br s, 2H), 7.98 (s, 1H), 7.79 (dd, J = 8.5, 1.0 Hz, 1H), 7.53 (s, 1H), 7.50 (s, 1H), 6.79 (d, J = 8.5 Hz, 1H), 2.01 (s, 3H), 1.69 (s, 4H), 1.33 (s, 6H), 1.25 (s, 3H), 1.23 (s, 3H). FAB-MS m/z: 378 $[M + H]^+$.

*1-(3,5,5,8,8-Pentamethyl-5,6,7,8-tetrahydronaphthalen-2-yl)-2-trifluoromethyl-1H-benzoimidazole-5-carboxylic Acid (**6c**).* To a solution of **16c** (50 mg, 0.11 mmol) in MeOH (1.0 mL) and THF (2.0 mL) was added 2 N NaOH (1.0 mL). The reaction mixture was stirred at 60 °C for 1.0 h and then poured into 2 N HCl (2.0 mL) and extracted with EtOAc (3 × 40 mL). The organic layer was collected, washed with brine (10 mL) and H_2O (10 mL), dried over $MgSO_4$, and evaporated under reduced pressure. The residue was recrystallized from EtOAc/*n*-hexane to yield 21 mg of **6c** as a colorless powder (43%). Mp: 235.8–237.1 °C. ^{1}H NMR (300 MHz, $CDCl_3$) δ: 8.75 (d, J = 1.5 Hz, 1H), 8.15 (dd, J = 8.5, 1.5 Hz, 1H), 7.30 (s, 1H), 7.21 (s, 1H), 7.15 (d, J = 9.5 Hz, 1H), 1.91 (s, 3H), 1.74 (s, 4H), 1.36 (s, 6H), 1.25 (s, 6H). FAB-MS m/z: 431 $[M + H]^+$. Anal. Calcd for $C_{24}H_{25}F_3N_2O_2$: C, 66.96; H, 5.85; N, 6.51. Found: C, 66.93; H, 6.11; N, 6.41.

*2-Oxo-1-(3,5,5,8,8-pentamethyl-5,6,7,8-tetrahydro-2-naphthyl)-2,3-dihydro-1H-benzoimidazole-5-carboxylic Acid (**6d**).* To a solution of **16d** (120 mg, 0.30 mmol) in MeOH (10 mL) was added 2 N NaOH (10 mL). The reaction mixture was stirred at 60 °C for 30 min, poured into 1 N HCl (20 mL), and extracted with EtOAc (2 × 30 mL). The organic layer was washed with H_2O (40 mL) and brine (30 mL), dried over $MgSO_4$, and evaporated under reduced pressure to yield 110 mg of **6d** as a pale yellow solid (qy). The residue was recrystallized from EtOAc/*n*-hexane to yield 45 mg of **6d** as a colorless powder. Mp: > 295 °C; ^{1}H NMR (300 MHz, DMSO-d_6) δ: 12.69 (br s, 1H), 11.29 (s, 1H), 7.64 (dd, J = 8.0, 1.5 Hz, 1H), 7.59 (d, J = 1.5 Hz, 1H), 7.39 (s, 1H), 7.26 (s, 1H), 6.63 (d, J = 8.0 Hz, 1H), 2.01 (s, 3H), 1.68 (s, 4H), 1.31 (s, 3H), 1.30 (s, 3H), 1.24 (s, 3H), 1.23 (s, 3H); IR (KBr): 2959–2926 (OH), 1712 (CO), 1685 (CO) cm^{-1}. FAB-MS m/z: 379 $[M + H]^+$. Anal. Calcd for $C_{23}H_{26}N_2O_3 \cdot 1/4H_2O$: C, 72.13; H, 6.97; N, 7.31. Found: C, 72.40; H, 7.05; N, 7.18.

*1-(3,5,5,8,8-Pentamethyl-5,6,7,8-tetrahydro-2-naphthyl)-2-thioxo-2,3-dihydro-1H-benzoimidazole-5-carboxylic Acid (**6e**).* To a solution of **16e** (120 mg, 0.30 mmol) in MeOH (3.0 mL) was added 2 N NaOH (3.0 mL). The reaction mixture was stirred at 60 °C for 15 min, poured into 2 N HCl (30 mL), and extracted with EtOAc (2 × 20 mL). The organic layer was washed with H_2O (2 × 30 mL) and brine (30 mL), dried over $MgSO_4$, and evaporated under reduced pressure to yield 100 mg of **6e** as a pale yellow solid (86%). The residue was recrystallized from EtOAc/*n*-hexane to yield 90 mg of **6e** as pale yellow needles. Mp: > 295.0 °C. ^{1}H NMR (300 MHz, DMSO-d_6) δ: 13.20 (br s, 1H), 12.91 (br s, 1H), 7.76 (dd, J = 8.5, 1.5 Hz, 1H), 7.75 (d, J = 1.5 Hz, 1H), 7.41 (s, 1H), 7.24 (s, 1H), 6.68 (d, J = 8.5 Hz, 1H), 1.95 (s, 3H), 1.68 (s, 4H), 1.33 (s, 3H), 1.32 (s, 3H), 1.23 (s, 3H), 1.23 (s, 3H). IR (KBr): 3056 (NH), 2962–2923 (OH), 1693 (CO) cm^{-1}. FAB-MS m/z: 395 $[M + H]^+$. Anal. Calcd for $C_{23}H_{26}N_2O_2S \cdot 1/2H_2O$: C, 68.48; H, 6.74; N, 6.94. Found: C, 68.39; H, 6.63; N, 6.82.

*1-(3,5,5,8,8-Pentamethyl-5,6,7,8-tetrahydronaphthalen-2-yl)-1H-indole-5-carboxylic Acid Methyl Ester (**19**).* To a solution of **17** (1.0 g, 3.6 mmol) and **18** (530 mg, 3.0 mmol) in dry toluene (4.0 mL) were added CuI (28 mg, 0.15 mmol), K_3PO_4 (1.3 g, 6.3 mmol), KI (600 mg, 3.6 mmol), and *N*,*N*′-dimethylethylenediamine (65 μL, 0.60 mmol). The reaction mixture was refluxed at 160 °C for 2.5 h under microwave irradiation, filtered through Celite, and evaporated

dx.doi.org/10.1021/jm400033f | J. Med. Chem. 2013, 56, 1865–1877

under reduced pressure. The residue was purified by flash column chromatography (EtOAc:*n*-hexane = 1:40) to yield 89 mg of **19** as yellow crystals (7.9%). ^{1}H NMR (300 MHz, $CDCl_3$) δ: 8.47 (d, J = 2.0 Hz, 1H), 7.88 (dd, J = 9.0, 2.0 Hz, 1H), 7.28 (s, 1H), 7.25 (d, J = 3.0 Hz, 1H), 7.23 (s, 1H), 7.09 (d, J = 9.0 Hz, 1H), 6.75 (d, J = 3.0 Hz, 1H), 3.95 (s, 3H), 2.00 (s, 3H), 1.74 (s, 1H), 1.36 (s, 6H), 1.28 (s, 6H).

1-(3,5,5,8,8-Pentamethyl-5,6,7,8-tetrahydronaphthalen-2-yl)-1H-indole-5-carboxylic Acid (7). To a solution of **19** (66 mg, 0.18 mmol) in MeOH (2.0 mL) and THF (1.0 mL) was added 2 N NaOH (2.0 mL). The reaction mixture was stirred at 60 °C for 1.5 h, poured into 2 N HCl (2.0 mL), and extracted with EtOAc (3 × 40 mL). The organic layer was collected, washed with brine (20 mL), dried over $MgSO_4$, and evaporated under reduced pressure to yield 58 mg of **7** (92%). The residue was recrystallized from EtOAc/*n*-hexane to yield 10 mg of **7** as a colorless powder. Mp: 244.0−245.0 °C. HPLC: 33 min; >95% purity (MeOH:$AcONH_4$(aq) = 80:20). ^{1}H NMR (300 MHz, DMSO) δ: 12.5 (s, 1H), 8.47 (d, J = 2.0 Hz, 1H), 7.74 (dd, J = 9.0, 2.0 Hz, 1H), 7.58 (d, J = 3.0 Hz, 1H), 7.41 (s, 1H), 7.26 (s, 1H), 7.09 (d, J = 9.0 Hz, 1H), 6.79 (d, J = 3.0 Hz, 1H), 1.94 (s, 3H), 1.68 (s, 4H), 1.31 (s, 6H), 1.24 (s, 6H). FAB-MS m/z: 362 $[M + H]^+$. Anal. Calcd for $C_{24}H_{27}NO_2 \cdot 1/4H_2O$: C, 78.76; H, 7.57; N, 3.83. Found: C, 78.60; H, 7.36; N, 3.93.

Luciferase Reporter Gene Assay. *Culture of COS-1 Cells.* COS-1 cells were maintained in Dulbecco's modified Eagle's medium supplemented with 10% FBS, $NaHCO_3$ (1.0 g), L-glutamine (0.292 g), penicillin (25 000 units), and streptomycin (25 000 μg) in a humidified atmosphere of 5% CO_2 in air at 37 °C.

Luciferase Reporter Gene Assay. Luciferase reporter gene assays were performed using COS-1 cells transfected with three kinds of vectors: each receptor subtype, a luciferase reporter gene under the control of the appropriate RXR response element, and secreted alkaline phosphatase (SEAP) gene[33] as a background. CRBPII-tk-Luc, tk-TREPII-Luc, tk-PPREx3-Luc, and tk-rBARx3-Luc reporters were used as RXR, RAR, PPAR, and LXR response elements, respectively. The amounts of each receptor subtype and response element were 1.0 and 4.0 μg, respectively. Transfection was performed with QIA Effectene transfection reagent according to the supplier's protocol. In the case of heterodimer assay, RXRα (0.5 μg), each partner receptor (PPARγ or LXRα, 0.5 μg), and the partner response element (4.0 μg) were transfected into COS-1 cells as described above. Test compound solutions (DMSO concentration below 1%) were added to the suspension of transfected cells, which were seeded at about 2.0×10^4 cells/well in 96-well white plates. After incubation in a humidified atmosphere of 5% CO_2 at 37 °C for 18 h, 25 μL of the medium was used for analyzing SEAP activities, and the remaining cells were used for luciferase reporter gene assays with a Steady-Glo luciferase assay system (Promega) according to the supplier's protocol. The luciferase activities were normalized using SEAP activities. The assays were carried out in triplicate three times.

Production and Purification of RXRα Protein. Production and purification of recombinant RXRα protein were done using GATEWAY technology.[34,35] Destination vectors were generated by insertion of human RXRα DNA (Ultimate Human ORF Clone, Invitrogen)[36] into a pDEST17 vector (Invitrogen) and were transformed into *Escherichia coli* BL21-AI cells (Invitrogen) by means of LR reaction. These cells were used as expression clones. The expression clones were cultured in LB medium containing 100 μg/mL ampicillin at 37 °C with shaking until the OD_{600} reached 0.6−1.0 and then were diluted to OD 0.1 at 600 nm. After addition of 0.2% L-arabinose and 0.1% glucose to the culture during the exponential phase of growth (OD 0.4 at 600 nm), cells were cultured for 2 h and then harvested. The cell pellets were resuspended in Lysis buffer (50 mM Tris-HCl, pH 7.5, 0.15 M NaCl, 0.1% SDS, 1.0% Triton X-100, 1 mM PMSF) at 4 °C. The RXR protein was purified using a His GraviTrap column (GE Healthcare)[37] to give 2.2 mg/L pure protein in the culture medium.

Fluorescence Polarization Assay. Fluorescein-labeled cofactor peptides were purchased from Life Technologies. Assays were performed in 96-well half-area black plates (Greiner) in a final volume of 40 μL. All reagents were diluted in phosphate buffer (50 mM sodium phosphate pH 7.2, 154 mM NaCl, 1 mM dithiothreitol, 1 mM EDTA, 0.01% NP40), and the final DMSO concentration in the assay mixtures was adjusted to 1%. The mixtures containing fluorescein-labeled cofactor peptide, RXRα, and various RXR ligands in phosphate buffer were incubated for 1 h at 25 °C. The fluorescence polarization of the mixtures was measured at an excitation wavelength of 485 nm and an emission wavelength of 535 nm. Fluorescence polarization measurements were made with a TECAN Polarion. Fluorescence polarization is the ratio of the difference between the intensities of parallel and perpendicularly polarized fluorescent light to the total light intensity.

Electrostatic Potential Fields and Molecular Docking. The crystal structure of human RXRα−ligand binding domain was retrieved from the Brookhaven Protein Data Bank (http://www.rcsb.org/pdb/Welcome.do). Polar hydrogen atoms were added to both the protein and the ligand. United atom Kollman charges were assigned for the protein. The 3D structures of ligands used for the docking study were constructed by using Spartan (Wave function, Inc.). After semi-empirical pm3 calculations, 6-31G* ab initio calculations were performed to find the lowest energy conformers. The electrostatic potential fields (ESP) were drawn with Spartan. The AutoDock4.2 molecular docking program[32] was employed by using a genetic algorithm with local search (GALS). One hundred individual GA runs, 150 chromosomes, a crossover ratio of 0.80, a rate of gene mutation of 0.02, and an elitism ratio of 0.10 were used for each ligand. The grid box was created with dimensions of 40 × 40 × 40 Å^3, which encloses the original ligand. Molfeat (FiatLux Co., Tokyo, Japan) was used for molecular modeling.

In Vivo Assays. *General.* All experiments were conducted in accordance with the Guidelines for Animal Experiments at Okayama University Advanced Science Research Center, and all procedures were approved by the Animal Research Control Committee of Okayama University.

Measurement of Serum Concentration of Test Compounds after Oral Administration at 30 mg/kg to Mice. Groups of six-week-old ICR male mice (n = 6−9 in each) were treated with solutions of test compound 30 mg/kg (1% ethanol and 0.5% CMC in distilled water) at a volume of 10 mL/kg of body weight by oral administration. At the indicated times, 0.6 mL of blood was taken from the inferior vena cava under diethyl ether anesthesia. Each blood sample was centrifuged at 1900*g* for 5 min at rt. To 100 μL of the resulting plasma were added 100 μL of ice-cold 5 mM ammonium acetate solution (adjusted with acetic acid to pH 5.0) and 1 mL of ice-cold ethyl acetate. The resulting mixture was vortexed for 30 s, kept at room temperature for 10 min, and centrifuged at 1900*g* for 30 s at room temperature. An 800 μL aliquot of the ethyl acetate phase was removed and concentrated to dryness in a centrifugal evaporator. To the resulting residue was added 100 μL of HPLC-grade methanol. This solution was directly subjected to HPLC analysis, and the concentration of each compound was determined from the peak area of the sample with reference to a calibration plot obtained with the authentic compound.

HPLC Conditions. The HPLC system used in this study was a Shimadzu liquid chromatographic system (Kyoto, Japan) consisting of an SCL-10A system controller, LC-10AD pump, SPD-10AV UV−vis spectrophotometric detector, SIL-10AD autoinjector, CTO-10A column oven, DGU-14A degasser, and C-R7A Chromatopac. The samples (each 20 μL) were injected using a refrigerated autosampler kept at 10 °C. The chromatographic analyses were carried out on an Inertsil ODS-3 (4.6 i.d. × 250 mm, 5 μm, GL Sciences, Tokyo, Japan) kept at 40 °C, using methanol:33.3 mM ammonium acetate (adjusted with acetic acid to pH 5.0) (85:15, v/v) as the mobile phase. The flow rate was 0.7 mL/min and the absorbance was monitored at 280 nm.

Observation of Side Effects after Once-Daily Oral Administration at 30 mg/kg for 7 Consecutive Days in Male ICR Mice. Six- to seven-week-old male ICR mice were purchased from Charles River Laboratories Japan, Inc. After arrival of the animals, all were group-housed and acclimated to the colony for 1 or 2 days before the experiment. Before the experiment, they were housed with four mice per cage, with free access to water and chow pellets in a light (12 h on, 8:00 a.m. /12 h off, 8:00 p.m.), temperature (23 ± 1 °C), and relative

humidity (50 ± 20%) controlled environment. Before experiments, mice were assigned to experimental groups so as to minimize the variance between groups based on the measured weight [four per cage (17 × 33 × 15 cm^3)]. Body weight was measured at approximately 10:00 a.m. every day for 7 days before dosing. Mice were administered orally with a solution of test compound at a dose of 30 mg/kg or with the vehicle [1% ethanol and 0.5% carboxymethyl cellulose (CMC) in distilled water] at a volume of 10 mL/kg of animal at approximately 10:00 a.m. every day for 7 days. On the final day of dosing, animals were fasted from 17:00 p.m. and given water ad libitum. On the next day, at approximately 10:00 a.m., animals were weighed and anesthetized with diethyl ether. Blood and liver were removed immediately, and the liver was weighed. Approximately 1 mL of blood in an Eppendorf sample tube was centrifuged to afford a serum sample. Each blood sample was centrifuged at 1900*g* for 5 min at rt.

Observation of Side Effects after Once-Daily Oral Administration at 30 mg/kg for 28 Consecutive Days in SD Rats. Four-week-old male and female SD rats were purchased from Charles River Laboratories Japan, Inc. After arrival of the rats, all were group-housed and acclimated to the colony for 6 (male) or 7 (female) days before the experiment. Before the experiment, they were housed with two rats per cage, with free access to water and chow pellets in a light (12 h on, 8:00 a.m./12 h off, 8:00 p.m.), temperature (23 ± 1 °C), and relative humidity (50 ± 20%)-controlled environment. Before experiments, rats were assigned to experimental groups so as to minimize the variance between groups based on the measured weight [two per cage (25.0 × 41.5 × 19.0 cm^3)]. Body weight was measured at approximately 10:00 a.m. every day for 28 days before dosing. Rats were administered orally with a solution of test compound at a dose of 30 mg/kg or with the vehicle (1% ethanol and 0.5% CMC in distilled water) at a volume of 5 mL/kg of animal at approximately 10:00 a.m. every day for 28 days. On the final day of dosing, animals were fasted from 17:00 p.m. and given water ad libitum. On the next day, at approximately 10:00 a.m., animals were weighed and anesthetized with isoflurane. Blood, liver, brain, kidney, spleen, and testis (male only) were removed immediately. The liver, brain, kidney, spleen, and testis were weighed and frozen with liquid nitrogen. Approximately 10 mL of blood in a centrifuge tube was centrifuged at 2000*g* for 10 min at 4 °C to obtain a serum sample.

Evaluation of Blood Glucose-Lowering Activities in KK-A^y Mice. Type 2 diabetic KK-A^y mice, in which the A^y allele at the agouti locus had been transferred to the inbred KK strain by repetitive backcrossing, were used as the congenic strain. The introduction of the A^y allele caused DM and massive hereditary obesity. Four-week-old male KK-A^y mice were purchased from CLEA Japan Inc. The KK-A^y mice were allowed free access to solid food and tap water. After arrival of the animals, all were group-housed and acclimated to the colony for 6 weeks before the experiment. Before the experiment, they were housed with one mouse per cage, with free access to water and chow pellets in a light (12 h on, 8:00 a.m./12 h off, 8:00 p.m.), temperature (23 ± 1 °C), and relative humidity (50 ± 20%) controlled environment. Before experiments, mice were assigned to experimental groups so as to minimize the variance between groups based on the blood glucose level [one per cage (17 × 33 × 15 cm^3)]. Body weight was measured at approximately 10:00 a.m. every day for 14 days before dosing. Mice were administered orally with a solution of test compound at a dose of 10 mg/kg or with the vehicle (1% ethanol and 0.5% CMC in distilled water) at a volume of 10 mL/kg of animal at approximately 10:00 a.m. every day for 14 days. At day 15, an oral glucose tolerance test (OGTT) was performed, and animals were fasted from 17:00 p.m. and given water ad libitum. On the next day, at approximately 10:00 a.m., animals were weighed and anesthetized with diethyl ether. Blood was removed immediately and centrifuged in an Eppendorf sample tube to obtain serum. Each blood sample was centrifuged at 1900*g* for 5 min at rt. Samples for measurements of fed blood glucose level were taken from the tail vein of the mice, and glucose was measured by using the glucose oxidase method (Medisafe-mini, TERUMO, Tokyo, Japan).

Measurements of Blood Parameters. Aspartate aminotransferase (AST), alanine aminotransferase (ALT), γ-glutamyl transpeptidase (γ-GTP), alkaline phosphatase (ALP), creatinine (CRE), blood urea nitrogen (BUN), triglyceride (TG), total cholesterol (TCHO), and glucose (GLU) were measured by using a Fuji Dry Chem system (Dry Chem 4000 V, Fuji Medical Co., Tokyo, Japan).

Oral Glucose Tolerance Test. KK-A^y mice treated with each compound for 14 days were fasted for 17 h and orally given glucose solution (100 mg glucose in 1 mL distilled water) at a dose of 1 g/kg body weight. At 0, 15, 30, 45, 60, 90, and 120 min after the glucose loading, blood glucose level was measured as described above.

■ ASSOCIATED CONTENT

Ⓢ Supporting Information

HPLC charts and in vitro and in vivo data are described. This information is available free of charge via the Internet at http://pubs.acs.org.

■ AUTHOR INFORMATION

Corresponding Author

*Tel/Fax: +81-(0)86-251-7963. E-mail: kakuta@pharm.okayama-u.ac.jp.

Author Contributions

H.K. conceived and designed the project. F.O., N.Y., R.S. and M.H. synthesized compounds. F.O., S.Y., and Y.O. performed reporter gene assays. M.M. prepared plasmids. H.N. prepared RXR proteins. S.Y. performed cofactor recruitment assays. A.T. and H.K. performed HPLC analysis. F.O., M.N., K.K., T.K., K.K., Y.F., C.F., Y.Y., H.Y., and H.K. performed in vivo experiments. The manuscript was written by F.O., A.T., and H.K.

Notes

The authors declare no competing financial interest.

■ ACKNOWLEDGMENTS

We thank Dr. Miyachi (Okayama University) for kindly providing TIPP-703 and carba-T0901317. We also thank Dr. Kagechika (Tokyo Medical and Dental University) for kindly providing PA452. The authors are also grateful to Prof. Yoshio Naomoto, Dr. Takuya Fukazawa (Kawasaki Medical School), and Mrs. Kaori Endo-Umeda (Nihon University) for preparing plasmids. The authors gratefully thank Division of Instrumental Analysis, Okayama University for the NMR measurements. This work was supported by Health and Labour Science research grants for Research on Seeds for Publicly Essential Drugs and Medical Devices (23080401) from the Ministry of Health, Labour, and Welfare of Japan. We also thank the Ministry of Education, Science, Culture and Sports of Japan, Takeda Science Foundation and "Top Young Researcher Award of Okayama University for 2011" for financial support.

■ ABBREVIATIONS USED

RXR, retinoid X receptor; RAR, retinoic acid receptor; LXR, liver X receptor; PPAR, peroxisome proliferator-activated receptors; qy, quantitative yield; TFAA, trifluoroacetic anhydride; TFA, trifluoroacetic acid; TEA, triethylamine; DCE, 1,2-dichloroethane; DBU, 1,8-diazabicyclo[5.4.0]undec-7-ene; DMEDA, *N*,*N*′-dimethylethylenediamine; Asn, asparagine; Gly, glycine; TG, triglyceride; TCHO, total cholesterol; AST, alanine aminotransferase; ALT, aspartate aminotransferase; γ-GTP, γ-glutamyltranspeptidase; ALP, alkaline phosphatase; CRE, creatinine; BUN, blood urea nitrogen.

■ REFERENCES

(1) Svensson, S.; Ostberg, T.; Jacobsson, M.; Norström, C.; Stefansson, K.; Hallén, D.; Johansson, I. C.; Zachrisson, K.; Ogg, D.; Jendeberg, L. Crystal structure of the heterodimeric complex of LXRα

and RXRβ ligand-binding domains in a fully agonistic conformation. *EMBO J.* **2003**, *22*, 4625−4633.
(2) de Lera, A. R.; Bourguet, W.; Altucci, L.; Gronemeyer, H. Design of selective nuclear receptor modulators: RAR and RXR as a case study. *Nat. Rev. Drug Discovery* **2007**, *6*, 811−820.
(3) Mangelsdorf, D. J.; Evans, R. M. The RXR heterodimers and orphan receptors. *Cell* **1995**, *83*, 841−850.
(4) Su, C. G.; Wen, X.; Bailey, S. T.; Jiang, W.; Rangwala, S. M.; Keilbaugh, S. A.; Flanigan, A.; Murthy, S.; Lazar, M. A.; Wu, G. D. A novel therapy for colitis utilizing PPARγ ligands to inhibit the epithelial inflammatory response. *J. Clin. Invest.* **1999**, *104*, 383−389.
(5) Chao, E. Y.; Caravella, J. A.; Watson, M. A.; Campobasso, N.; Ghisletti, S.; Billin, A. N.; Galardi, C.; Wang, P.; Laffitte, B. A.; Iannone, M. A.; Goodwin, B. J.; Nichols, J. A.; Parks, D. J.; Stewart, E.; Wiethe, R. W.; Williams, S. P.; Smallwood, A.; Pearce, K. H.; Glass, C. K.; Willson, T. M.; Zuercher, W. J.; Collins, J. L. Structure-guided design of *N*-phenyl tertiary amines as transrepression-selective liver X receptor modulators with anti-inflammatory activity. *J. Med. Chem.* **2008**, *51*, 5758−5765.
(6) Pascual, G.; Fong, A. L.; Ogawa, S.; Gamliel, A.; Li, A. C.; Perissi, V.; Rose, D. W.; Willson, T. M.; Rosenfeld, M. G.; Glass, C. K. A SUMOylation-dependent pathway mediates transrepression of inflammatory response genes by PPARγ. *Nature* **2005**, *437*, 759−763.
(7) Mitro, N.; Mak, P. A.; Vargas, L.; Godio, C.; Hampton, E.; Molteni, V.; Kreusch, A.; Saez, E. The nuclear receptor LXR is a glucose sensor. *Nature* **2007**, *445*, 219−223.
(8) Commerford, S. R.; Vargas, L.; Dorfman, S. E.; Mitro, N.; Rocheford, E. C.; Mak, P. A.; Li, X.; Kennedy, P.; Mullarkey, T. L.; Saez, E. Dissection of the insulin-sensitizing effect of liver X receptor ligands. *Mol. Endocrinol.* **2007**, *21*, 3002−3012.
(9) Joseph, S. B.; Castrillo, A.; Laffitte, B. A.; Mangelsdorf, D. J.; Tontonoz, P. Reciprocal regulation of inflammation and lipid metabolism by liver X receptors. *Nat. Med.* **2003**, *9*, 213−219.
(10) Fowler, A. J.; Sheu, M. Y.; Schmuth, M.; Kao, J.; Fluhr, J. W.; Rhein, L.; Collins, J. L.; Willson, T. M.; Mangelsdorf, D. J.; Elias, P. M.; Feingold, K. R. Liver X receptor activators display antiinflammatory activity in irritant and allergic contact dermatitis models: Liver-X-receptor-specific inhibition of inflammation and primary cytokine production. *J. Invest. Dermatol.* **2003**, *120*, 246−255.
(11) Shulman, A. I.; Larson, C.; Mangelsdorf, D. J.; Ranganathan, R. Structural determinants of allosteric ligand activation in RXR heterodimers. *Cell* **2004**, *116*, 417−429.
(12) Gniadecki, R.; Assaf, C.; Bagot, M.; Dummer, R.; Duvic, M.; Knobler, R.; Ranki, A.; Schwandt, P.; Whittaker, S. The optimal use of bexarotene in cutaneous T-cell lymphoma. *Br. J. Dermatol.* **2007**, *157*, 433−440.
(13) Boehm, M. F.; Zhang, L.; Badea, B. A.; White, S. K.; Mais, D. E.; Berger, E.; Suto, C. M.; Goldman, M. E.; Heyman, R. A. Synthesis and structure−activity relationships of novel retinoid X receptor-selective retinoids. *J. Med. Chem.* **1994**, *37*, 2930−2941.
(14) Fujii, S.; Ohsawa, F.; Yamada, S.; Shinozaki, R.; Fukai, R.; Makishima, M.; Enomoto, S.; Tai, A.; Kakuta, H. Modification at the acidic domain of RXR agonists has little effect on permissive RXR heterodimer activation. *Bioorg. Med. Chem. Lett.* **2010**, *20*, 5139−5142.
(15) Takamatsu, K.; Takano, A.; Yakushiji, N.; Morohashi, K.; Morishita, K.; Matsuura, N.; Makishima, M.; Tai, A.; Sasaki, K.; Kakuta, H. The first potent subtype-selective retinoid X receptor (RXR) agonist possessing a 3-isopropoxy-4-isopropylphenylamino moiety, NEt-3IP (RXRα/β-dual agonist). *ChemMedChem* **2008**, *3*, 780−787.
(16) Kakuta, H.; Yakushiji, N.; Shinozaki, R.; Ohsawa, F.; Yamada, S.; Ohta, Y.; Kawata, K.; Nakayama, M.; Hagaya, M.; Fujiwara, C.; Makishima, K.; Uno, S.; Tai, A.; Maehara, A.; Nakayama, M.; Oohashi, T.; Yasui, H.; Yoshikawa, Y. RXR partial agonist CBt-PMN exerts therapeutic effects on type 2 diabetes without the side effects of RXR full agonists. *ACS Med. Chem. Lett.* **2012**, *3*, 427−432.
(17) Pogenberg, V.; Guichou, J. F.; Vivat-Hannah, V.; Kammerer, S.; Pérez, E.; Germain, P.; de Lera, A. R.; Gronemeyer, H.; Royer, C. A.; Bourguet, W. Characterization of the interaction between retinoic acid receptor/retinoid X receptor (RAR/RXR) heterodimers and transcriptional coactivators through structural and fluorescence anisotropystudies. *J. Biol. Chem.* **2005**, *280*, 1625−1633.
(18) Li, X.; Hansen, P. A.; Xi, L.; Chandraratna, R. A.; Burant, C. F. Distinct mechanisms of glucose lowering by specific agonists for peroxisomal proliferator activated receptor gamma and retinoic acid X receptors. *J. Biol. Chem.* **2005**, *280*, 38317−38327.
(19) Lenhard, J. M.; Lancaster, M. E.; Paulik, M. A.; Weiel, J. E.; Binz, J. G.; Sundseth, S. S.; Gaskill, B. A.; Lightfoot, R. M.; Brown, H. R. The RXR agonist LG100268 causes hepatomegaly, improves glycaemic control and decreases cardiovascular risk and cachexia in diabetic mice suffering from pancreatic beta-cell dysfunction. *Diabetologia* **1999**, *42*, 545−554.
(20) Davies, P. J.; Berry, S. A.; Shipley, G. L.; Eckel, R. H.; Hennuyer, N.; Crombie, D. L.; Ogilvie, K. M.; Peinado-Onsurbe, J.; Fievet, C.; Leibowitz, M. D.; Heyman, R. A.; Auwerx, J. Metabolic effects of rexinoids: Tissue-specific regulation of lipoprotein lipase activity. *Mol. Pharmacol.* **2001**, *59*, 170−176.
(21) Ohsawa, F.; Morishita, K.; Yamada, S.; Makishima, M.; Kakuta, H. Modification at the lipophilic domain of RXR agonists differentially influences activation of RXR heterodimers. *ACS Med. Chem. Lett.* **2010**, *1*, 521−525.
(22) Kakuta, H.; Ohsawa, F.; Yamada, S.; Makishima, M.; Tai, A.; Yasui, H.; Yoshikawa, Y. Feasibility of structural modification of RXR agonists to separate blood glucose-lowering action from adverse effects: Studies in KK-A^y type 2 diabetes model mice. *Biol. Pharm. Bull.* **2012**, *35*, 629−633.
(23) Qing, F. L.; Yue, X. J. A novel synthesis of 9,13-di-*cis* double bonds locked retinoids. *Tetrahedron Lett.* **1997**, *38*, 8067−8070.
(24) Germain, P.; Staels, B.; Dacquet, C.; Spedding, M.; Laudet, V. Overview of nomenclature of nuclear receptors. *Pharmacol. Rev.* **2006**, *58*, 685−704.
(25) Oberfield, J. L.; Collins, J. L.; Holmes, C. P.; Goreham, D. M.; Cooper, J. P.; Cobb, J. E.; Lenhard, J. M.; Hull-Ryde, E. A.; Mohr, C. P.; Blanchard, S. G.; Parks, D. J.; Moore, L. B.; Lehmann, J. M.; Plunket, K.; Miller, A. B.; Milburn, M. V.; Kliewer, S. A.; Willson, T. M. A peroxisome proliferator-activated receptor gamma ligand inhibits adipocyte differentiation. *Proc. Natl. Acad. Sci. U. S. A.* **1999**, *96*, 6102−6106.
(26) Egea, P. F.; Mitschler, A.; Rochel, N.; Ruff, M.; Chambon, P.; Moras, D. Crystal structure of the human RXRalpha ligand-binding domain bound to its natural ligand: 9-*cis* Retinoic acid. *EMBO J.* **2000**, *19*, 2592−2601.
(27) Lévy-Bimbot, M.; Major, G.; Courilleau, D.; Blondeau, J.; Lévi, Y. Tetrabromobisphenol-A disrupts thyroid hormone receptor alpha function in vitro: Use of fluorescence polarization to assay corepressor and coactivator peptide binding. *Chemosphere* **2012**, *87*, 782−788.
(28) Ozers, M. S.; Ervin, K. M.; Steffen, C. L.; Fronczak, J. A.; Lebakken, C. S.; Carnahan, K. A.; Lowery, R. G.; Burke, T. J. Analysis of ligand-dependent recruitment of coactivator peptides to estrogen receptor using fluorescence polarization. *Mol. Endcrinol.* **2005**, *19*, 25−34.
(29) Stafslien, D. K.; Vedvik, K. L.; Rosier, T.; Ozers, M. S. Analysis of ligand-dependent recruitment of coactivator peptides to RXRβ in a time-resolved fluorescence resonance energy transfer assay. *Mol. Cell. Endocrinol.* **2007**, *264*, 82−89.
(30) Ghosh, J. C.; Yang, X.; Zhang, A.; Lambert, M. H.; Li, H.; Xu, H. E.; Chen, J. D. Interactions that determine the assembly of a retinoid X receptor/corepressor complex. *Proc. Natl. Acad. Sci. U. S. A.* **2002**, *99*, 5842−5847.
(31) Takahashi, B.; Ohta, K.; Kawachi, E.; Fukasawa, H.; Hashimoto, Y.; Kagechika, H. Novel retinoid X receptor antagonists: Specific inhibition of retinoid synergism in RXR−RAR heterodimer actions. *J. Med. Chem.* **2002**, *45*, 3327−3330.
(32) Morris, G. M.; Huey, R.; Lindstrom, W.; Sanner, M. F.; Belew, R. K.; Goodsell, D. S.; Olson, A. J. AutoDock4 and AutoDockTools4: Automated docking with selective receptor flexibility. *J. Comput. Chem.* **2009**, *30*, 2785−2791.

(33) Kain, S. R. Use of secreted alkaline phosphatase as a reporter of gene expression in mammalian cells. *Methods Mol. Biol.* **1997**, *63*, 49–60.
(34) Landy, A. Dynamic, structural, and regulatory aspects of lambda site-specific recombination. *Annu. Rev. Biochem.* **1989**, *58*, 913–949.
(35) Walhout, A. J.; Temple, G. F.; Brasch, M. A.; Hartley, J. L.; Lorson, M. A.; van den Heuvel, S.; Vidal, M. GATEWAY recombinational cloning: Application to the cloning of large numbers of open reading frames or ORFeomes. *Methods Enzymol.* **2000**, *328*, 575–592.
(36) Liang, F.; Matrubutham, U.; Parvizi, B.; Yen, J.; Duan, D.; Mirchandani, J.; Hashima, S.; Nguyen, U.; Ubil, E.; Loewenheim, J.; Yu, X.; Sipes, S.; Williams, W.; Wang, L.; Bennett, R.; Carrino, J. ORFDB: An information resource linking scientific content to a high-quality open reading frame (ORF) collection. *Nucleic Acids Res.* **2004**, *32*, D595–D599.
(37) Hengen, P. Purification of His-Tag fusion proteins from *Escherichia coli*. *Trends Biochem. Sci.* **1995**, *20*, 285–286.

Supporting Information

Mechanism of RXR partial agonistic action of CBt-PMN and structural development to increase potency

Fuminori Ohsawa[†], *Shoya Yamada*[†‡], *Nobumasa Yakushiji*[†], *Ryosuke Shinozaki*[†], *Mariko Nakayama*[†], *Kohei Kawata*[†], *Manabu Hagaya*[†], *Toshiki Kobayashi*[†], *Kazutaka Kohara*[†], *Yuuki Furusawa*[†], *Chisa Fujiwara*[†], *Yui Ohta*[†], *Makoto Makishima*[§], *Hirotaka Naitou*[¶], *Akihiro Tai*[#], *Yutaka Yoshikawa*[◊], *Hiroyuki Yasui*[◊], *and Hiroki Kakuta*[†]*

†Division of Pharmaceutical Sciences, Okayama University Graduate School of Medicine, Dentistry and Pharmaceutical Sciences, 1-1-1, Tsushima-Naka, Okayama 700-8530, Japan.

‡Research Fellowship Division, Japan Society for the Promotion of Science, Sumitomo-Ichibancho FS Bldg., 8 Ichibancho, Chiyoda-ku, Tokyo 102-8472, Japan.

§Division of Biochemistry, Department of Biomedical Sciences, Nihon University School of Medicine, 30-1 Oyaguchi-kamicho, Itabashi-ku, Tokyo 173-8610, Japan.

¶Graduate School of Nutritional and Environmental Sciences, University of Shizuoka, 52-1 Yada, Suruga-ku, Shizuoka 422-8526, Japan.

#Faculty of Life and Environmental Sciences, Prefectural University of Hiroshima, 562 Nanatsuka-Cho, Shobara, Hiroshima 727-0023, Japan.

◊Kyoto Pharmaceutical University, 5 Nakauchi-cho, Misasagi, Yamashina-ku, Kyoto 607-8414, Japan.

E-mail: kakuta@pharm.okayama-u.ac.jp

Contents: